protocol (QIAamp DNA Blood Mini Kit; Qiagen, Gaithersburg, MD, USA).

MLPA

MLPA screening of all of *Dystrophin* exons employed two sets of probes (SALSA-MLPA P034-A2 and P035-A2) (MRC Holland, Amsterdam, The Netherlands).

DNA Sequencing

Direct DNA sequencing was performed using an automated DNA Sequencer (model 3130; Applied Biosystems, Forster City, CA, USA) for cases where MLPA found an apparent deletion of only one exon or no exon deletion/duplication at all.

In Silico Splicing Analysis of Nucleotide Mutations

Due to the absence of RNA specimens in our possession, we decided to perform in silico analysis to predict the effect of all nucleotide mutations on splicing. We used ESEfinder 3.0 (Cartegni et al., 2003) software (http://cb.utdallas.edu/cgi-bin/tools/ESE3/esefinder.cgi) that analyzes five exonic splicing enhancer (ESE) motifs (SF2/ASF, SF2/ASF (IgM-BRCA1), SC35, SRp40, and SRp55) to predict disruption of exonic splicing enhancer motifs by analyzing the splicing score created by the mutations as compared with the score in the wild-type exon sequence. In addition, we also analyzed the possibility of cryptic splice site using Human Splicing Finder software version 2.4.1 (www.umd.be/HSF/4DACTION/input_SSF).

RESULTS

Clinical Diagnoses and Patients Characteristics

All patients were clinically examined and diagnosed as having DMD/BMD based on their clinical features and creatine kinase (CK) levels (Table 1). Among these patients, only 18 had an identifiable family history of DMD (51.4%). All patients were positive for the Gower's sign and showed an average increase in serum CK levels by 22.8 ± 14.6 times (mean 10002.3 ± 4576.3 U/L), except those within the early stage of disease progression (65-F59 and 66-F60).

Dystrophin Mutation of the Malaysian DMD/BMD Cohort

This study included 35 DMD/BMD patients (Table 1). We identified five different types of disease-causing *Dystrophin* mutations: exonic deletions in 27 patients, exonic duplications in 2, nonsense in 3, missense in 2, and nucleotide deletions in 2. Two patients showed closely spaced combined mutations. They are patient 43-F41 with two concurrent nonsense mutations in exon 8 (c.701C→A and c.745C→T), which we reported in detail elsewhere (Rani et al., 2011), and patient 55-F51 with closely spaced missense mutation and nucleotide deletion (c.4741G→T and c.4742delA).

Mutations frequently clustered in two hotspots: 62.8% (22 out of 35) were localized within the distal hotspot. Two out of 30 (6%) deletion cases were in-frame (41-F39 and 45-F43, exons 8–19 and 3–13, respectively) but resulted in DMD phenotype.

In Silico Splicing Analyses

Mutations in our patients' cohort that underwent this analysis are the missense in patients 37-F35 and 55-F51, nonsense in patients 38-F36, 43-F41, and 49-F47, and nucleotide deletion in patients 55-F51 and 73-F63. Among them are patients with double nonsense in one exon (43-F41) and missense coupled by single-nucleotide deletion in one exon (55-F51), of which we analyzed them as combined events or separately.

We found that c.701C→A in patient 43-F41 decreases the best-hit scores in 2 out of 5 analyzed ESE motifs, SF2/ASF and SF2/ASF (IgM-BRCA1), by 0.14 and 0.16, respectively. Our in silico analyses did not show any effects of other nucleotide mutations on either ESE motifs or splice sites (raw data not shown).

DISCUSSION

A few studies have reported screening of selected *Dystrophin* exons only for deletions among Malaysian patients (Thong et al., 2005; Marini et al., 2008). This report is the first comprehensive molecular analysis of *Dystrophin* mutations among Malaysian DMD/BMD patients. We suggested that direct sequencing of additional exons could be done if MLPA could not identify any mutations. Although cDNA analyses could be an alternative, genomic DNA analyses are still preferable due to its practical reasons and use in molecular diagnosis with direct clinical relevance to patient/family counseling. Our data fit in a diverse spectrum of mutations.

We have also noted in this study that MLPA does improve the diagnostic technique, especially in detecting small mutations (patients 55-F51 and 73-F63).

Two of our patients showed DMD phenotype despite harboring in-frame deletions (41-F39 and 45-F43). The two in-frame deletions were located in the N-terminus of dystrophin. Thus, the most likely explanation for the

Table 1. Genotypes and phenotypes of Malaysian DMD/BMD patients in this study.

Patient ID	Genotypes		Age (year)	Onset (year)	Clinical information				Phenotype
	Mutations	Type			CK U/l	FH	Best current motor ability	Lower limb muscle	
1-F1	Del e43–52	Out	8	7	8540	Y	Waddling gait	Calf hypertrophy	DMD
3-F2	Del e44–51	Out	8	7	12690	N	Unstable gait	Calf hypertrophy	DMD
5-F4	Del e46–52	Out	12	5	6430	N	Bed-ridden	Contracture reflexes depressed	DMD
6-F5	Del e46–50	Out	8	3	10000	Y	Waddling gait	Calf hypertrophy	DMD
10-F9	Del e46–50	Out	7	5	4354	Y	Frequent falling, difficulties climbing stairs	Mild limb hyperextensibility	DMD
12-F11	Del e45	Out	9	5	Unknown	Y	Abnormal gait	Muscle weakness	DMD
13-F13	Del e46–53	Out	8	5	5794	Y	Gross motor development delay	Progressive muscle weakness	DMD
15-F14	Del e45–52	Out	9	6	2149	Y	Abnormal gait	Lower limb weakness, calf hypertrophy	DMD
17-F16	Del e46	Out	8	7	8880	N	Abnormal gait and frequent falling	Weakness, reflex negative	DMD
18-F17	Del e48–54	Out	5.5	4	7355	Y	Waddling gait, not able to stand up	Wasting the muscle bulk, calf muscle pseudohypertrophy	DMD
25-F23	Del e46–50	Out	7.5	5	8450	N	Waddling gait	Calf hypertrophy	DMD
26-F24	Del e16–17	Out	7	7	10260	N	Waddling gait	Calf pseudohypertrophy	DMD
27-F25	Del e50	Out	7	6	11770	N	Waddling gait	Calf pseudohypertrophy	DMD
28-F26	Del e18–32	Out	16	8	>10000	N	Wheelchair bound	Muscle wasting	DMD
30-F28	Del e45–54	Out	9	6	12170	N	Wheelchair bound	Small muscle bulk	DMD
33-F31	Del e8–30	Out	9	7	13325	N	Tip-toe gait	Calf pseudohypertrophy and tendon reflex absent	DMD
37-F35	c.8810A> G;p.E2937R (e59)	MS	8	5	18114	N	Waddling gait	Muscle weakness more of lower limbs, no tendons response	DMD
38-F36	c.3709A> T;p.K1237X (e27)*	NS	9	7	11456	N	Waddling gait	Progressive loss of muscles, calf pseudohypertrophy	DMD
39-F37	Del e44	Out	4.5	4	25320	Y	Frequent falling, not able to stand up	Calf pseudohypertrophy	DMD
40-F38	Del e 49–51	In	7	6	4363	Y	Still able to walk	Calf pseudohypertrophy	BMD
41-F39	Del e8–19	In	6	4	24590	Y	Wheelchair bound	Calf pseudohypertrophy and tendon reflex absent	DMD
43-F41	c.701C> A; p.S234X and c.745C> T;p.Q249X (e8)	NS	16	6	5408	N	Wheelchair bound	Calf pseudohypertrophy	DMD
45-F43	Del e3–13	In	7	5	9000	Y	Wheelchair bound	Calf pseudohypertrophy	DMD
49-F47	c.10171C> T;p.R3391X (e70)	NS	3	3	7000	Y	Tip-toe walking	Calf hypertrophy, lumbar lordosis, and hypotonic lower limbs	DMD
50-F48	Del e8–11	Out	7	6	Unknown	N	Frequent falling, difficulties climbing stairs	Calf pseudohypertrophy, oreflexia	DMD
51-F49	Del e49–50	Out	8	6	8076	Y	Waddling gait	Calf pseudohypertrophy	DMD
53-F50	Del e48–54	Out	6.5	6	18,104	N	Waddling gait, difficulty climbing stairs	Calf pseudohypertrophy	DMD
55-F51	c.4741G> T;p.M1580I and c.4742delA;p. N1581MFsX1583*	MS and Out	17	6	8440	Y	Bed-ridden	Muscle weakness	DMD
59-F54	Del e14–17	Out	10	8	6000	N	Sitting, shuttling	Weakness, calf hypertrophy	DMD
60-F55	Dup e11	Out	8	2	2466	Y	Bottom shuffling	Progressive weekness of both lower limb muscles	DMD
65-F59	Del e17–43	Out	6	5	162	N	Waddling gait	Bilateral calf swelling	DMD
66-F60	Del e3–43	Out	7	7	313	N	Waddling gait	Calf pseudohypertrophy	DMD
71-F61	Dup e45	Out	11	7	13310	N	Wheel chair bound	Weakness of lower limbs	DMD
73-F63	c.6804DelACAA	Out	8	7	11920	Y	Waddling gait	Bilateral lower limb weakness	DMD
74-F64	Del e45–50	Out	7	7	>10000	N	Not able to run or climb stairs	Calf pseudohypertrophy	DMD

e, exon; Out, out-of-frame; In, in-frame; NS, Nonsense; MS, Missense; CK, creatinine kinase level; FH, family history; Y, yes; N, no. Gower's sign was positive in all the cases. *Novel as of 18 September 2012

more severe phenotype in these two patients is a probable disruption of the actin binding domain (Muntoni et al., 1994; Cutiongco et al., 1995). Another reason might be that exon skipping has occurred at the RNA level, resulting in the skipping of these exons or creation of cryptic splice sites (Shiga et al., 1997; Melis et al., 1998; Ginjaar et al., 2000). Meanwhile, the presence of multiple mutations as possible phenotype modifiers, which have not been detected in the DNA of these two cases could not be excluded (Rani et al., 2011).

Our in silico analyses found that one mutation in exon 8 (c.701C→A) of patient 43-F41 altered the best-hit scores of two ESE motifs. However, it is difficult to postulate that this alteration may lead to changes in the splicing of exon 8. The effects of this nucleotide change on the ESE motif scores are still less than that of the classical example of exon skipping event in SMN2 exon 7 (Cartegni et al., 2003). Our analyses of SMN1/SMN2 exon 7 showed that the C→T change decreased the best-hit scores in 4 out of 5 analyzed ESE motifs: SF2/ASF, SF2/ASF (IgM-BRCA1), SC35, and SRp40, by 1.23, 0.28, 1.73, and 0.23, respectively.

Our analyses showed that exon 50 followed by exon 49 were the two most frequently deleted exons among Malaysian patients. This has further informed therapeutic studies, especially those focusing on targeted exon skipping (Takeshima et al., 2006; van Deutekom et al., 2007). In order to rescue the phenotype of at least 24% of Malaysian patients with DMD, skipping of exon 45 could be suggested.

In conclusion, we showed for the first time comprehensive clinical and molecular genetic findings in Malaysian patients with DMD/BMD. We found that MLPA coupled with further direct sequencing of 16 selected exons may increase the detection rate of *Dystrophin* mutation. Our second finding of closely spaced nucleotide changes implied that multiple *Dystrophin* mutations among DMD/BMD patients may be more frequent than previously thought.

ACKNOWLEDGMENTS

We would like to thank the clinicians, patients, and patients' families for their cooperation in this study. We also express our sincerest gratitude to Assoc. Prof. Dr. Zafarina Zainuddin of USM School of Health Sciences for her help and support.

Declaration of interest: The authors report no conflicts of interest. The authors alone are responsible for the content and writing of the paper.

This work was supported by Research University Grants 1001/PPSP/812058, 1001/PPSP/812048, and 1001/PPSP/812072 from Universiti Sains Malaysia. Rani A. Qawee is the recipient of the Universiti Sains Malaysia Fellowship for Doctoral course.

REFERENCES

Beggs, A. H., Koenig, M., Boyce, F. M., & Kunkel, L. M. (1990). Detection of 98% of DMD/BMD gene deletions by polymerase chain reaction. *Hum Genet, 86*, 45–48.

Cartegni, L., Wang, J., Zhu, Z., Zhang, M. Q., & Krainer, A. R. (2003). ESEfinder: A web resource to identify exonic splicing enhancers. *Nucleic Acids Res, 31*, 3568–3571.

Chamberlain, J. S., Gibbs, R. A., Ranier, J. E., Nguyen, P. N., & Caskey, C. T. (1988). Deletion screening of the Duchenne muscular dystrophy locus via multiplex DNA amplification. *Nucleic Acids Res, 16*, 11141–11156.

Cutiongco, E. M., Padilla, C. D., Takenaka, K., Yamasaki, Y., Matsuo, M., & Nishio, H. (1995). More deletions in the 5' region than in the central region of the dystrophin gene were identified among Filipino Duchenne and Becker muscular dystrophy patients. *Am J Med Genet, 59*, 266–267.

Ginjaar, I. B., Kneppers, A. L., v d Meulen, J. D., Anderson, L. V., Bremmer-Bout, M., van Deutekom, J. C., Weegenaar, J., den Dunnen, J. T., & Bakker, E. (2000). Dystrophin nonsense mutation induces different levels of exon 29 skipping and leads to variable phenotypes within one BMD family. *Eur J Hum Genet, 8*, 793–796.

Lai, K. K., Lo, I. F., Tong, T. M., Cheng, L. Y., & Lam, S. T. (2006). Detecting exon deletions and duplications of the DMD gene using Multiplex Ligation-dependent Probe Amplification (MLPA). *Clin Biochem, 39*, 367–372.

Lalic, T., Vossen, R. H., Coffa, J., Schouten, J. P., Guc-Scekic, M., Radivojevic, D., Djurisic, M., Breuning, M. H., White, S. J., & den Dunnen, J. T. (2005). Deletion and duplication screening in the DMD gene using MLPA. *Eur J Hum Genet, 13*, 1231–1234.

Marini, M., Salmi, A. A., Watihayati, M. S., MD, S. M., Zahri, M. K., Hoh, B. P., Ankathil, R., Lai, P. S., & Zilfalil, B. A. (2008). Screening of dystrophin gene deletions in Malaysian patients with Duchenne muscular dystrophy. *Med J Malaysia, 63*, 31–34.

Melis, M. A., Muntoni, F., Cau, M., Loi, D., Puddu, A., Boccone, L., Mateddu, A., Cianchetti, C., & Cao, A. (1998). Novel nonsense mutation (C→A nt 10512) in exon 72 of dystrophin gene leading to exon skipping in a patient with a mild dystrophinopathy. *Hum Mutat*, 11(Suppl 1), S137–S138.

Muntoni, F., Gobbi, P., Sewry, C., Sherratt, T., Taylor, J., Sandhu, S. K., Abbs, S., Roberts, R., Hodgson, S. V., Bobrow, M., Dubowitz, V. (1994). Deletions in the 5' region of dystrophin and resulting phenotypes. *J Med Genet, 31*, 843–847.

Rani, A. Q., Malueka, R. G., Sasongko, T. H., Awano, H., Lee, T., Yagi, M., Zilfalil, B. A., Salmi, A. B., Takeshima, Y., Zabidi-Hussin, Z. A., & Matsuo, M. (2011). Two closely spaced nonsense mutations in the DMD gene in a Malaysian family. *Mol Genet Metab, 103*, 303–304.

Shiga, N., Takeshima, Y., Sakamoto, H., Inoue, K., Yokota, Y., Yokoyama, M., & Matsuo, M. (1997). Disruption of the splicing enhancer sequence within exon 27 of the dystrophin gene by a nonsense mutation induces partial skipping of the exon and is responsible for Becker muscular dystrophy. *J Clin Invest, 100*, 2204–2210.

Takeshima, Y., Yagi, M., Okizuka, Y., Awano, H., Zhang, Z., Yamauchi, Y., Nishio, H., & Matsuo, M. (2010). Mutation spectrum of the dystrophin gene in 442 Duchenne/Becker

muscular dystrophy cases from one Japanese referral center. *J Hum Genet, 55*, 379–388.

Takeshima, Y., Yagi, M., Wada, H., Ishibashi, K., Nishiyama, A., Kakumoto, M., Sakaeda, T., Saura, R., Okumura, K., & Matsuo, M. (2006). Intravenous infusion of an antisense oligonucleotide results in exon skipping in muscle dystrophin mRNA of Duchenne muscular dystrophy. *Pediatr Res, 59*, 690–694.

Thong, M. K., Bazlin, R. I., & Wong, K. T. (2005). Diagnosis and management of Duchenne muscular dystrophy in a developing country over a 10-year period. *Dev Med Child Neurol, 47*, 474–477.

van Deutekom, J. C., Janson, A. A., Ginjaar, I. B., Frankhuizen, W. S., Aartsma-Rus, A., Bremmer-Bout, M., den Dunnen, J. T., Koop, K., van der Kooi, A. J., Goemans, N. M., de Kimpe, S. J., Ekhart, P. F., Venneker, E. H., Platenburg, G. J., Verschuuren, J. J., & van Ommen, G. J. (2007). Local dystrophin restoration with antisense oligonucleotide PRO051. *N Engl J Med, 357*, 2677–2686.

Journal of Human Genetics (2012), 1–7

www.nature.com/jhg

ORIGINAL ARTICLE

Molecular characterization of an X(p21.2;q28) chromosomal inversion in a Duchenne muscular dystrophy patient with mental retardation reveals a novel long non-coding gene on Xq28

Thi Hoai Thu Tran[1,3,4], Zhujun Zhang[1,3,5], Mariko Yagi[1], Tomoko Lee[1], Hiroyuki Awano[1], Atsushi Nishida[1,6], Takeshi Okinaga[2], Yasuhiro Takeshima[1] and Masafumi Matsuo[1,6]

Duchenne muscular dystrophy (DMD) is the most common inherited muscular disease and is characterized by progressive muscle wasting. DMD is caused by mutations in the *dystrophin* gene on Xp21.2. One-third of DMD cases are complicated by mental retardation, but the pathogenesis of this is unknown. We have identified an intrachromosomal inversion, inv(X)(p21.2;q28) in a DMD patient with mental retardation. We hypothesized that a gene responsible for the mental retardation in this patient would be disrupted by the inversion. We localized the inversion break point by analysis of *dystrophin* complementary DNA (cDNA) and fluorescence *in situ* hybridization. We used 5′ and 3′ rapid amplification of cDNA ends to extend the known transcripts, and reverse transcription-PCR to analyze tissue-specific expression. The patient's *dystrophin* cDNA was separated into two fragments between exons 18 and 19. Exon 19 was dislocated to the long arm of the X-chromosome. We identified a novel 109-bp sequence transcribed upstream of exon 19, and a 576-bp sequence including a poly(A) tract transcribed downstream of exon 18. Combining the two novel sequences, we identified a novel gene, named *KUCG1*, which comprises three exons spanning 50 kb on Xq28. The 685-bp transcript has no open-reading frame, classifying it as a long non-coding RNA. *KUCG1* mRNA was identified in brain. We cloned a novel long non-coding gene from a chromosomal break point. It was supposed that this gene may have a role in causing mental retardation in the index case.
Journal of Human Genetics advance online publication, 6 December 2012; doi:10.1038/jhg.2012.131

Keywords: dystrophin; long non-coding gene; mental retardation

INTRODUCTION

Duchenne muscular dystrophy (DMD) is the most common inherited muscle disease affecting approximately one in 3500 males and is characterized by progressive muscle wasting during childhood. DMD shows muscle dystrophin deficiency because of mutations in the *dystrophin* gene that comprises 79 exons spanning >2500 kb on chromosome Xp21.2.[1] Mutations in the *dystrophin* gene range from single-nucleotide changes to chromosomal abnormalities (http://www.dmd.nl/).[2] Deletions encompassing one or more exons of the *dystrophin* gene are the most common cause of DMD and account for ~60% of mutations.[3] Disastrous mutations such as an out-of-frame deletion or nonsense mutation result in severe DMD.[4] DMD is complicated by mental retardation in one-third of patients.[5] Many studies have been conducted to elucidate the pathogenic mechanism of this complicating mental retardation. There are now several reports describing that mutations at the 3′ end of the *dystrophin* gene are related to complication with mental retardation.[6,7]

In a small portion of DMD patients, gross chromosomal rearrangements have been reported as the cause of dystrophin deficiency. In fact, a huge intrachromosomal deletion showing contiguous gene deletion syndrome was used to clone the *dystrophin* gene.[8] Intrachromosomal inversions have been identified in DMD.[9,10] X-autosome translocations involving the *dystrophin* gene have also been identified in a limited number of DMD patients.[11,12]

Disease-associated chromosomal rearrangements have been frequently used as a starting point in the elucidation of congenital

[1]Department of Pediatrics, Kobe University Graduate School of Medicine, Kobe, Japan and [2]Department of Developmental Medicine (Pediatrics), Osaka University Graduate School of Medicine, Osaka, Japan
[3]These authors contributed equally to this work.
[4]Current address: Department of Pediatrics, Medical University of Pham Ngoc Thach, Ho Chi Minh City, Vietnam.
[5]Current address: Department of Pathology, Nankai University School of Medicine, Nankai University, Tianjin, People's Republic of China.
[6]Current address: Department of Medical Rehabilitation, Faculty of Rehabilitation, Kobegakuin University, Kobe, Japan.
Correspondence: Professor M Matsuo, Department of Medical Rehabilitation, Faculty of Rehabilitation, Kobegakuin University, 518 Arise, Ikawadani-cho, Nishi-ku, Kobe, Hyogo 6512180, Japan.
E-mail: mmatsuo@reha.kobegakuin.ac.jp or matsuo@kobe-u.ac.jp
Received 18 August 2012; revised 26 September 2012; accepted 10 October 2012

disorders. Disrupted X-chromosomal genes are even more promising in this respect as they often represent knockouts.[10,13] In one DMD patient with complicating mental retardation, for example, an intrachromosomal inversion led to the identification of a Ras-like GTPase gene that causes mental retardation.[9] In addition, >20 genes have been identified by studying balanced X-chromosome rearrangements.[14]

The genes for X-linked mental retardation are largely unknown.[14–16] In a series of 442 Japanese mutations in the *dystrophin* gene, we have described a karyotype of 46,Y,inv (X)(p21.2;q28) to be the cause of one case of DMD.[2] This case was complicated with moderate mental retardation and it is thought very likely that the inversion disrupts one of the >40 genes responsible for mental retardation at Xq28.[17]

A diverse population of non-protein-coding RNAs has been reported in the human genome.[18,19] Long non-coding RNAs (lncRNAs), defined as greater than 200 nucleotides (nt) in length,[20] have a wide range of functions, including the regulation of transcription, RNA editing and organelle biogenesis.[19,21,22] It has been suggested that a subset of lncRNAs could contribute to neurological disorders when they become dysregulated.[23]

In this study, we characterized an intrachromosomal inversion inv(X)(p21.2;q28). We identified a novel long non-coding gene named *KUCG1* at the break point on Xq28. As this gene was expressed in the brain, we propose that disruption of the *KUCG1* gene may have a role in causing the mental retardation in the index case.

MATERIALS AND METHODS

Patient

The index patient is a 3-year-old Japanese boy. He is the first child of healthy, non-consanguineous, Japanese parents. Family history was unremarkable. When he was born at term, blood sampling was performed because of birth asphyxia. Unexpectedly, his serum creatine kinase level was highly elevated (25 510 $IU l^{-1}$; normal: <270 $IU l^{-1}$). He walked unassisted at the age of 15 months. As the high creatine kinase level persisted, a muscle biopsy was conducted at the age of 2 years to examine dystrophin expression. Dystrophin staining using monoclonal antibodies to three different domains revealed no reactive material in his skeletal muscle, confirming the diagnosis of DMD. He was referred to Kobe University Hospital for a genetic diagnosis (KUCG481). At the age of 3 years, his serum creatine kinase was 21 776 $IU l^{-1}$. His growth parameters were normal but he displayed moderate mental retardation (developmental quotient: 40). Brain magnetic resonance imaging findings were normal. His karyotype has been described in our previous report as 46,Y, inv(X)(p21.2;q28).[2] The inversion was inherited through his mother (data not shown). The protocol for the following study was approved by the ethical committee of Kobe University School of Medicine.

Dystrophin mRNA analysis

RNA was isolated from biopsied skeletal muscle and analyzed by reverse transcription-PCR as described previously.[24,25] The full-length *dystrophin* complementary DNA (cDNA) was amplified as 10 separate fragments.[26] To identify the break point within the *dystrophin* cDNA, fragments encompassing exons 18 and 19 were amplified using different sets of primers. The ends of two separate *dystrophin* cDNAs were confirmed by PCR amplification using newly designed primers; a reverse primer on exon 18 and a forward primer on exon 19, respectively (Table 1).

PCR amplification

PCR amplification was performed in a total volume of 20 μl, containing 2 μl of cDNA, 2 μl of 10 × ExTaq buffer (Takara Bio, Inc., Shiga, Japan), 0.5 U of ExTaq polymerase (Takara Bio, Inc.), 500 nM of each primer and 250 μM deoxyribonucleotide triphosphates (Takara Bio, Inc.). Thirty-five cycles of amplification were performed on a Mastercycler Gradient PCR machine (Eppendorf, Hamburg, Germany) using the following conditions: initial denaturation at 94 °C for 5 min, subsequent denaturation at 94 °C for 0.5 min, annealing at 59 °C for 0.5 min and extension at 72 °C for 1 min. The conditions were sometimes slightly modified for optimization. For nested or semi-nested PCR, 2 μl of the first reaction mixture was used as the template for the second amplification. The amplified PCR products were electrophoresed on 2% agarose gels with a low-molecular weight DNA standard (φX174-Hae III digest; Takara Bio, Inc.) and stained with ethidium bromide.

Table 1 Primers used in this study

Primer name	*Primer sequence (5′-3′)*
Dystrophin cDNA	
Exon 18r	GCAGAGTCCTGAATTTGCAATC
Exon 19f	CATTCACCATCTGTTCCACCA
5′-RACE	
c24r	CAGCCATCCATTTCTTCAGG
c21r	TTGTCTGTAGCTCTTTCTCT
c20r	ACTGGCAGAATTCGATCCAC
3′-RACE	
c16f	CTGATCTAGAGGTACCGGATCC
c18f	GCAGAGTCCTGAATTTGCAATC
KUCG1 mRNA	
Bf	GGTGAACCCCTCAATGTAAG
Cr	CTCTTGTATTCGCTGCAGTG
Cr2	CAGCAAACTTGTACAGTTGC

Abbreviations: cDNA, complementary DNA; RACE, rapid amplification of cDNA ends.

Fluorescence *in situ* hybridization

Fluorescence *in situ* hybridization was conducted on metaphase spreads from the patients' lymphocytes with digoxigenin-labeled PCR product containing exons 18 or 19 of the *dystrophin* gene in combination with DXZ1 spectrum green probe for the X centromere (Vysis, Inc., Downers Grove, IL, USA). The exon 18 and 19 probes were detected by immunocytochemistry. This assay was carried out commercially by Mitsubishi Chemical Medience Co. (Tokyo, Japan).

5′-Rapid amplification of cDNA ends

5′-Rapid amplification of cDNA ends (RACE) was performed to obtain the 5′-end of the transcript using the 5′-RACE System Version 2 (Invitrogen, Carlsbad, CA, USA) according to the manufacturer's instructions, with primers specific for the *dystrophin* mRNA (Table 1). Total RNA isolated from the patient's skeletal muscle was reverse transcribed using a gene-specific primer (c24r) and SuperScript II, a derivative of Moloney Murine Leukemia Virus Reverse Transcriptase (Invitrogen). PCR amplification was then performed using Taq DNA polymerase (Takara Bio, Inc.), a nested gene-specific primer (c21r), and a deoxyinosine-containing anchor primer provided with the system. A nested amplification using an inner gene-specific primer (c20r) and the anchor primer from the provider was also performed.

3′-Rapid amplification of cDNA ends

3′-RACE was performed to obtain the 3′-end of the transcript using the 3′-RACE System Version 2 (Invitrogen) with primers specific for the *dystrophin* mRNA (Table 1). First-strand cDNA synthesis was initiated at the poly(A) tail of mRNA using the adapter primer from the provider. After first-strand cDNA synthesis, the original mRNA template was destroyed with *RNase* H. Amplification was performed using a gene-specific primer (c16f) and a universal amplification primer from the provider that targets the cDNA complementary to the 3′-end of the mRNA. A nested amplification using an inner gene-specific primer (c18f) and the anchor primer from the provider was also performed.

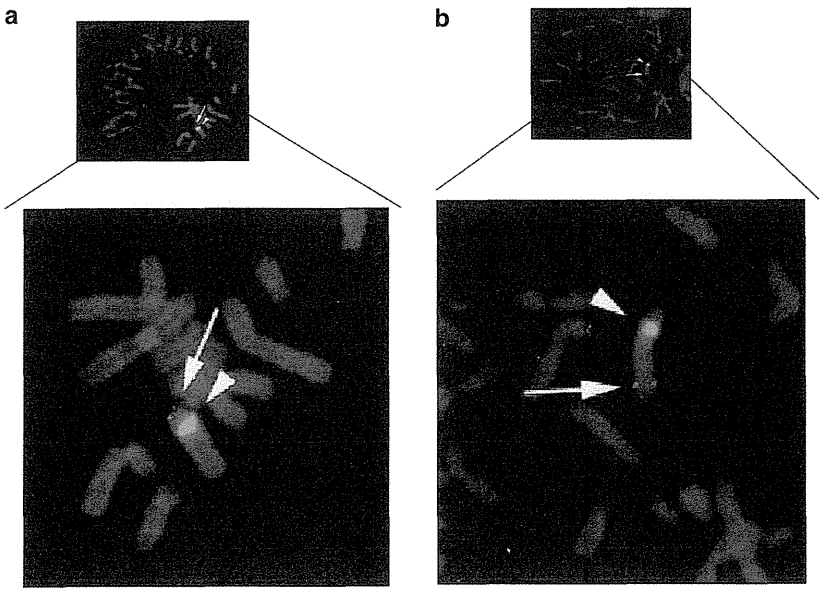

Figure 1 FISH analysis revealing disruption of the *dystrophin* gene. Results of FISH examination are shown with an enlarged panel (below). Centromeric signal is marked by arrowheads. (**a**) Exon 18 probe. Hybridization signals (arrow) are present on the short arm of the X-chromosome. (**b**) Exon 19 probe. Signals (arrow) are present on the long arm of the X-chromosome. A full color version of this figure is available at the *Journal of Human Genetics* journal online.

DNA sequencing

PCR-amplified bands were excised from the gel with a sharp razor blade, pooled and purified using a QIAGEN gel extraction kit (QIAGEN, Inc., Hilden, Germany) according to the manufacturer's instructions. Purified products were sequenced either directly or after subcloning into the pT7 Blue T-vector (Novagen, San Diego, CA, USA). DNA sequencing was performed using a BigDye 1.1 Terminator Cycle Sequencing kit (Applied Biosystems, Foster City, CA, USA) in a Mastercycler Gradient (Eppendorf). The DNA sequences were determined using an automated DNA sequencer (ABI 310; Applied Biosystems).

mRNA expression of KUCG1

The expression of the *KUCG1* transcript was examined by reverse transcription-PCR. Human total RNA from 21 tissues (adrenal gland, bone marrow, brain, colon, fetal brain, fetal liver, heart, kidney, liver, lung, lymphocytes, placenta, prostate, salivary gland, skeletal muscle, spinal cord, testis, thymus, thyroid gland, trachea and uterus) was obtained from a human total RNA Master Panel II (Clontech Laboratories, Inc., Mountain View, CA, USA). cDNA was synthesized as described previously[27] from 2.5 μg of each total RNA. The *KUCG1* transcript spanning exon 2 to exon 3 was amplified by semi-nested PCR using primers Bf and Cr2, then Bf and Cr1 (Table 1), yielding a 314-bp fragment.

To check the integrity and concentration of the cDNA, the glyceraldehyde-3-phosphate dehydrogenase gene was also reverse transcription-PCR amplified, as described previously.[28]

Database searches and multiple sequence alignments

Homology searching was performed using the National Center for Biotechnology Information BLAST program (http://blast.ncbi.nlm.nih.gov/Blast.cgi). The cloned 658-bp sequence was searched using NONCODE v3.0.[29] The core promoter of the *KUCG1* gene was analyzed using Genety X (Ver. 8.2.0) (GENETYX corporation, Tokyo, Japan).

RESULTS

We performed a molecular characterization of an intrachromosomal inversion in a DMD patient, inv(X)(p21.2;q28). We were able to amplify all 79 *dystrophin* exon-encompassing regions from the patient's genome (data not shown), indicating that the overall structure of the gene was intact. We examined the full-length *dystrophin* cDNA as 10 separate fragments. All the cDNA fragments could be obtained by PCR except one that covered exons 17 to 25 (data not shown). This suggested that the *dystrophin* cDNA was separated into two fragments; one from exons 1 to 18 and the other from exons 19 to 79 (data not shown). We used fluorescence *in situ* hybridization to confirm this. As expected, an exon 19 probe hybridized to the long arm of the X-chromosome, while an exon 18 probe hybridized to the short arm (Figure 1). We concluded that the exon 19 dislocation from the short arm to the long arm was the cause of DMD.

We were surprised the distal *dystrophin* cDNA (exons 19 to 78) could be PCR amplified, because this indicated that it formed a new fusion gene after dislocation. We, therefore, examined the full-length transcript using skeletal muscle RNA from the patient (Figure 2). We obtained a 5′-RACE product from exon 20, which contained 109 bp between the adapter and *dystrophin* exon 19 sequence (Figure 2). Homology searching of the identified sequence revealed that, although it did not match any known gene, it was identical to a portion of Xq28 (GenBank ID: NW001842413.1). The first nucleotide of the cloned sequence was 89,813 bp downstream from the melanoma antigen family A, 9 (*MAGEA9*) gene (Figure 3). Examination of the genomic sequence 3′ of the cloned 109-bp sequence revealed a GT dinucleotide, a splice donor consensus sequence (Figure 2). Although an AG dinucleotide-a consensus splice acceptor sequence was not present at the 5′-end, we did identify a TATA-box 5′-(ATATATAA CAATTTA)-3′, GC-box 5′-(TAAGGGCATACCCT)-3′ and CCAAT-box 5′-(CCTAGCCAATAG)-3′ at 168, 266 and 372 bp upstream of the cloned sequence, respectively (Figure 2). Additionally, a cap signal sequence (TCAGCAAC) was present 24 bp upstream. These characteristics indicated that the cloned sequence was the first exon of an unknown gene that is transcribed in the centromere-to-telomere direction. We concluded that, in the patient, the first exon of the

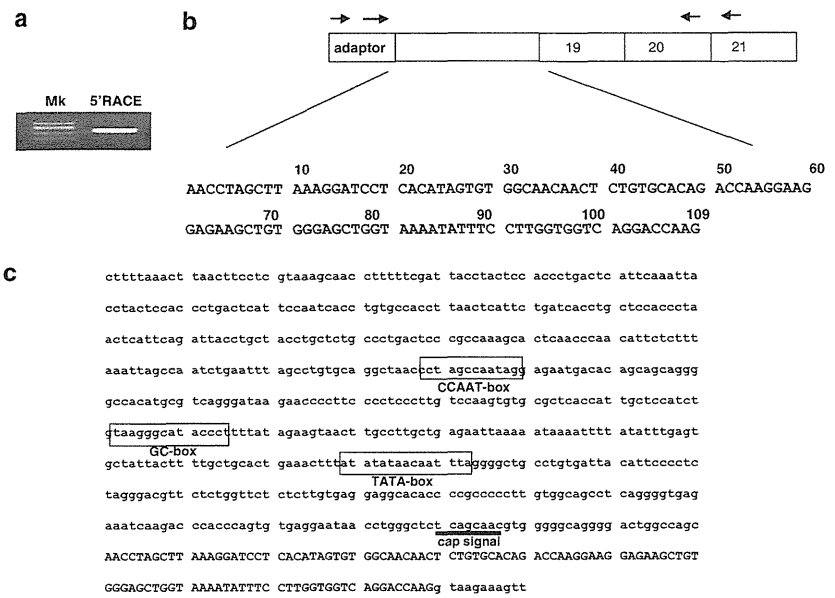

Figure 2 5′-RACE of *dystrophin* transcript. (**a**) Product of 5′-RACE of skeletal muscle RNA from the patient is shown (5′-RACE). Mk refers to ϕX174-*Hae III* molecular weight marker. (**b**) Schematic description of the amplified product. Numbered boxes indicate *dystrophin* exons. The open box indicates the novel 109-bp sequence. Arrows indicate primers used for PCR. (**c**) Part of Xq28 genomic sequence indicating the identified 109 nt (upper case). The boxed regions indicate the TATA-box, GC-box and CCAAT-box at 168, 266 and 372 bp upstream, respectively. A cap signal (thick underline) was identified 24 nt upstream of the 109-bp sequence.

unknown gene spliced to the dislocated part of the *dystrophin* gene, producing a chimeric *dystrophin* transcript.

To identify the rest of the novel gene, we conducted 3′-RACE using a primer in exon 16, and obtained one clear product (Figure 4). Sequencing of the amplified product revealed a 583-bp sequence inserted between *dystrophin* exon 18 and the adapter sequence (Figure 4). Homology searching revealed that this sequence, apart from the last seven 'A' nt, matched two separate regions of Xq28. The first 123 bp that were continuous with the 3′-end of exon 18 completely matched nt 148986563–148986685 and the last 453 bp matched nt 149008147–149008599 (NC 00023.10). The last nucleotide was located 4448 bp upstream of the melanoma antigen family A, 8 (*MAGEA8*) gene (Figure 3). Examination of the genomic sequences flanking the first 123 bp revealed consensus splice donor and acceptor sites at the 3′ and 5′ ends, respectively, indicating that it is an internal exon of an unknown gene. The last 453 bp had an AG dinucleotide immediately upstream but no GT dinucleotide downstream. Instead, a consensus polyadenylation signal (AATAAA) was identified 14 bp upstream of the 3′-end (Figure 4).[30] Considering the stretch of seven 'A's as part of a poly(A) tail, we concluded that the 453 bp sequence was the last exon of the unknown gene. The *dystrophin* promoter would produce a chimeric transcript comprising *dystrophin* exons 1–18 and two novel exons at the 3′-end.

Combining the results of 5′ and 3′-RACE, we had cloned a 685-bp-long transcript, the sequence of which we deposited in GenBank under the accession number JX283354. Homology searching did not reveal any transcript with significant similarity. The transcript had no significant open-reading frame, but because of its mRNA-like structure and length of >200 bp, we concluded that it was a novel lncRNA. We named it *KUCG1*. *KUCG1* spans nearly 50 kb on Xq28 and is located 9.0 kb downstream of *MAGEA9* and 4.4 kb upstream of *MAGEA8* (Figure 3). It has three exons separated by two introns (32 kb and 20 kb long, respectively). The site of recombination of the intrachromosomal inversion inv(X)(p21.2;q28) was intron 1. The inversion caused a head-to-tail fusion of *KUCG1* and *dystrophin* at the recombination sites. We searched for homologous lncRNAs using NONCODE v3.0,[29] but did not identify any significant matches. This indicated that *KUCG1* is a novel lncRNA. It was found that exon 3 of KUCG1 overlaps with the antisense transcript RP5-869M20.2, an lncRNA of unknown function (Figure 3).

We next examined the tissue-specific expression of *KUCG1* in humans. We amplified a fragment comprising exons 2 to 3 by reverse transcription-PCR of total RNA from 21 human tissues. The expected size product was obtained by semi-nested PCR from four tissues (lung, thyroid gland, brain and placenta), whereas no product was obtained from the other 17 tissues (Figure 5). Considering the brain expression of *KUCG1*, we consider that its disruption may be responsible for the moderate mental retardation in the index case.

DISCUSSION

In this report, we describe molecular characterization of an inverted X (p21.2;q28) chromosome in a patient with DMD and mental retardation. The inversion disrupted both the *dystrophin* gene, presumed to be the cause of the DMD, and a novel lncRNA, *KUCG1*, which may be the cause of the mental retardation. This is the third intrachromosomal inversion to be molecularly clarified in DMD,[9,10] but the first to disrupt unknown gene directly.

The *KUCG1* mRNA was detected in 4 out of 21 tissues: lung, thyroid gland, brain and placenta (Figure 5), indicating tissue-specific gene regulation despite the presence of three common consensus sequences in the promoter. The tissue-restricted expression and low expression level (semi-nested PCR was required to detect a product) could explain why this lncRNA has not been previously detected among the thousands of ncRNAs identified by high-throughput sequencing.[31]

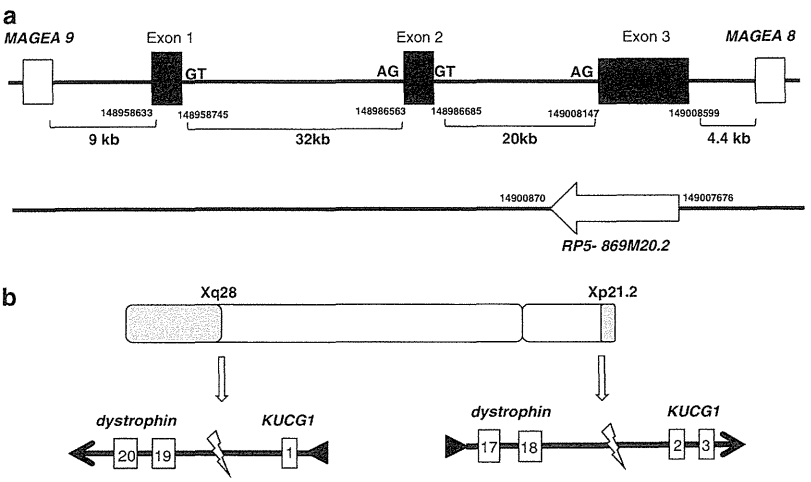

Figure 3 Schematic description of the gene and X-chromosome. (**a**) Schematic description of the *KUCG1* gene. The *KUCG1* gene that spans nearly 50 kb on Xq28 is transcribed in a centromere-to-telomere direction, and comprises three exons (black boxes) of 109, 123 and 453 bp, respectively. Numbers below the exons indicate the chromosomal nucleotide position according to GenBank NC00023.10. Introns 1 and 2 span 32 kb and 20 kb, respectively. *KUCG1* is located between *MAGEA9* and *MAGEA8* (open boxes). Another non-coding gene, *RP5-869M20.2* (ENSG00000230899.1) has been mapped to this region (nt 149007636–149009870) but is transcribed in the antisense direction (horizontal arrow). (**b**) Schematic description of the translocated X-chromosome schema of inv(X)(p21.2;q28) is described. At Xq28 intron 1 of the *KUCG 1* gene directly joined to intron 18 of the *dystrophin* gene. In contrast, intron 18 of the *dystrophin* gene joined to intron 1 of the *KUCG1* gene. Open and shaded boxes are normal and translocated parts of X-chromosome, respectively. Horizontal arrows and triangles indicate the direction and the promoter region of fused genes, respectively.

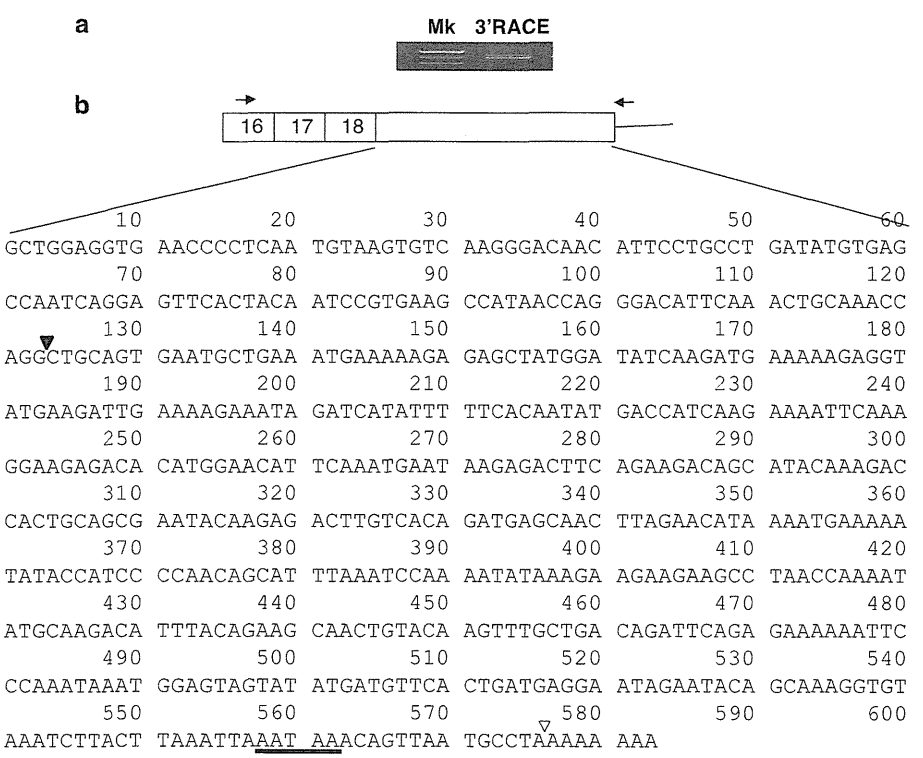

Figure 4 3′-RACE of *dystrophin* transcript. (**a**) Product of 3′-RACE of skeletal muscle RNA from the patient is shown (3′-RACE). Mk refers toϕX174-*Hae III* molecular weight marker. (**b**) Schematic description and sequence of the 3′-RACE product. *Dystrophin* exons are indicated as numbered open boxes. The product contained a 583-nt sequence (open box) downstream of *dystrophin* exon 18 (numbered box). The 583-nt sequence contains a polyadenylation signal (thick underline) followed by a short poly(A) tail (open triangle). The first 123 nt and the last 453 nt of the sequence (separated at the filled triangle) matched two separate regions on Xq28.

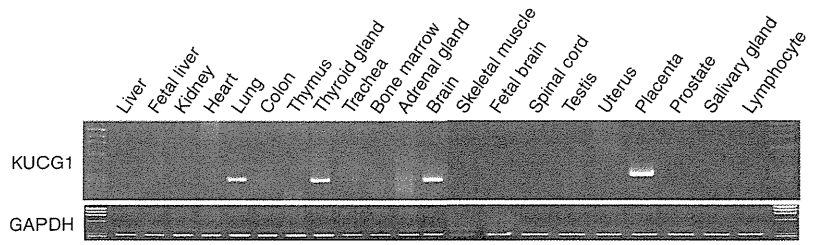

Figure 5 Tissue-specific expression of *KUCG1* mRNA. Products of reverse transcription-PCR amplification of *KUCG1* mRNA are shown. Reverse transcription-PCR amplification of 21 human tissues revealed a product in lung, thyroid gland, brain and placenta. The correct identity of the product was validated by sequencing. Glyceraldehyde-3-phosphate dehydrogenase (*GAPDH*) mRNA levels were used as a reference.

What is the function of the *KUCG1* gene? As it undergoes splicing, is >200 nt long, and contains features such as a poly(A) signal/tail, *KUCG1* can be considered an mRNA-like ncRNA.[32,33] lncRNAs have been shown to have key roles in imprinting control, immune responses and human disease;[20] for instance, an ncRNA cloned from a chromosomal inversion was recently demonstrated to cause autosomal dominant hypertension and brachydactyly (OMIM 112410).[34] In the central nervous system, the increasing variety of ncRNAs shown to be expressed has suggested a strong connection between ncRNAs and the complexity of the system.[35] Hundreds of lncRNAs have been shown to localize to specific neuroanatomical regions, cell types or subcellular compartments within the brain[36] and a subset of lncRNAs is likely to contribute to neurological disorders.[23] For instance, the levels of the linc-MD1 lncRNA are strongly reduced in DMD,[37] indicating a role for this lncRNA in the disease pathology of DMD.

The mechanism of action of lncRNAs is thought to involve direct binding to target sites on proteins and RNAs.[33,37] It is interesting that exon 3 of *KUCG1* overlaps with the antisense transcript *RP5-869M20.2*, an lncRNA of unknown function. It is possible that transcripts from *KUCG1* and *RP5-869M20.2* form a double-stranded RNA that has a particular physiological role.

As *KUCG1* is expressed in the brain, we suspect that its disruption is responsible for the moderate mental retardation in the index case. Although >40 genes responsible for X-linked mental retardation have been annotated to Xq28,[17] the gene(s) responsible for many cases of X-linked mental retardation remain unidentified.[14] To test whether *KUCG1* is responsible for other cases of X-linked mental retardation, we sequenced *KUCG1* in ten Japanese families with X-linked mental retardation for which no responsible gene mutation has been identified. No mutations were identified (data not shown). Although we have not provided direct evidence linking mental retardation to mutation of *KUCG1*, further studies of its function, and mutation analysis in other X-linked mental retardation families, is warranted.

CONFLICT OF INTEREST

The authors declare no conflict of interest.

ACKNOWLEDGEMENTS

We would like to thank Ms K Yoshikawa for her secretarial help. This work was supported by a Health and Labor Sciences Research Grant for Research on Psychiatric and Neurological Diseases and Mental Health, a Grant-in-Aid for Scientific Research grant (B) from the Japan Society for the Promotion of Science (MEXT/JSPS KAKENHI, grant number 24390267), and a research grant for Nervous and Mental Disorders from the Ministry of Health, Labor, and Welfare, Japan.

1 Ahn, A. H. & Kunkel, L. M. The structural and functional diversity of dystrophin. *Nat. Genet.* **3**, 283–291 (1993).
2 Takeshima, Y., Yagi, M., Okizuka, Y., Awano, H., Zhang, Z., Yamauchi, Y. *et al.* Mutation spectrum of the dystrophin gene in 442 Duchenne/Becker muscular dystrophy cases from one Japanese referral center. *J. Hum. Genet.* **55**, 379–388 (2010).
3 Koenig, M., Hoffman, E. P., Bertelson, C. J., Monaco, A. P., Feener, C. & Kunkel, L. M. Complete cloning of the Duchenne muscular dystrophy (DMD) cDNA and preliminary genomic organization of the DMD gene in normal and affected individuals. *Cell* **50**, 509–517 (1987).
4 Monaco, A. P., Bertelson, C. J., Liechti-Gallati, S., Moser, H. & Kunkel, L. M. An explanation for the phenotypic differences between patients bearing partial deletions of the DMD locus. *Genomics* **2**, 90–95 (1988).
5 Daoud, F., Candelario-Martinez, A., Billard, J. M., Avital, A., Khelfaoui, M., Rozenvald, Y. *et al.* Role of mental retardation-associated dystrophin-gene product Dp71 in excitatory synapse organization, synaptic plasticity and behavioral functions. *PLoS One* **4**, e6574 (2009).
6 Taylor, P. J., Betts, G. A., Maroulis, S., Gilissen, C., Pedersen, R. L., Mowat, D. R. *et al.* Dystrophin gene mutation location and the risk of cognitive impairment in Duchenne muscular dystrophy. *PLoS One* **5**, e8803 (2010).
7 Pane, M., Lombardo, M. E., Alfieri, P., D'Amico, A., Bianco, F., Vasco, G. *et al.* Attention deficit hyperactivity disorder and cognitive function in Duchenne muscular dystrophy: phenotype–genotype correlation. *J. Pediatr.* **161**, 705–709 (2012).
8 Kunkel, L, Hejtmancik, JF, Caskey, CT, Speer, A, Monaco, AP, Middlesworth, W *et al.* Analysis of deletions in DNA from patients with Becker and Duchenne muscular dystrophy. *Nature* **322**, 73–77 (1986).
9 Saito-Ohara, F., Fukuda, Y., Ito, M., Agarwala, K. L., Hayashi, M., Matsuo, M. *et al.* The Xq22 inversion break point interrupted a novel ras-like GTPase gene in a patient with Duchenne muscular dystrophy and profound mental retardation. *Am. J. Hum. Genet.* **71**, 637–645 (2002).
10 Bhat, S. S., Schmidt, K. R., Ladd, S., Kim, K. C., Schwartz, C. E., Simensen, R. J. *et al.* Disruption of DMD and deletion of ACSL4 causing developmental delay, hypotonia, and multiple congenital anomalies. *Cytogenet. Genome Res.* **112**, 170–175 (2006).
11 van Bakel, I., Holt, S., Craig, I. & Boyd, Y. Sequence analysis of the breakpoint regions of an X;5 translocation in a female with Duchenne muscular dystrophy. *Am. J. Hum. Genet.* **57**, 329–336 (1995).
12 Kalz-Fuller, B., Sleegers, E., Schwanitz, G. & Schubert, R. Characterisation, phenotypic manifestations and X-inactivation pattern in 14 patients with X-autosome translocations. *Clin. Genet.* **55**, 362–366 (1999).
13 Wheway, J. M., Yau, S. C., Nihalani, V., Ellis, D., Irving, M., Splitt, M. *et al.* A complex deletion-inversion-deletion event results in a chimeric IL1RAPL1-dystrophin transcript and a contiguous gene deletion syndrome. *J. Med. Genet.* **40**, 127–131 (2003).
14 Ropers, H. H. & Hamel, B. C. X-linked mental retardation. *Nat. Rev. Genet.* **6**, 46–57 (2005).
15 Raymond, F. L. X linked mental retardation: a clinical guide. *J. Med. Genet.* **43**, 193–200 (2006).
16 Tarpey, P. S., Smith, R., Pleasance, E., Whibley, A., Edkins, S., Hardy, C. *et al.* A systematic, large-scale resequencing screen of X-chromosome coding exons in mental retardation. *Nat. Genet.* **41**, 535–543 (2009).
17 Kolb-Kokocinski, A., Mehrle, A., Bechtel, S., Simpson, J. C., Kioschis, P., Wiemann, S. *et al.* The systematic functional characterisation of Xq28 genes prioritises candidate disease genes. *BMC Genomics* **7**, 29 (2006).
18 Amaral, P. P., Dinger, M. E., Mercer, T. R. & Mattick, J. S. The eukaryotic genome as an RNA machine. *Science* **319**, 1787–1789 (2008).
19 Derrien, T., Guigo, R. & Johnson, R. The long non-coding RNAs: a new (P)layer in the 'Dark Matter'. *Front. Genet.* **2**, 107 (2012).
20 Mercer, T. R., Dinger, M. E. & Mattick, J. S. Long non-coding RNAs: insights into functions. *Nat. Rev. Genet.* **10**, 155–159 (2009).
21 Mercer, T. R., Qureshi, I. A., Gokhan, S., Dinger, M. E., Li, G., Mattick, J. S. *et al.* Long noncoding RNAs in neuronal-glial fate specification and oligodendrocyte lineage maturation. *BMC Neurosci.* **11**, 14 (2010).
22 Taft, R. J., Pang, K. C., Mercer, T. R., Dinger, M. & Mattick, J. S. Non-coding RNAs: regulators of disease. *J. Pathol.* **220**, 126–139 (2010).

23 Niland, C. N., Merry, C. R. & Khalil, A. M. Emerging roles for long non-coding RNAs in cancer and neurological disorders. *Front. Genet.* **3,** 25 (2012).
24 Shiga, N., Takeshima, Y., Sakamoto, H., Inoue, K., Yokota, Y., Yokoyama, M. *et al.* Disruption of the splicing enhancer sequence within exon 27 of the dystrophin gene by a nonsense mutation induces partial skipping of the exon and is responsible for Becker muscular dystrophy. *J. Clin. Invest.* **100,** 2204–2210 (1997).
25 Kubokawa, I., Takeshima, Y., Ota, M., Enomoto, M., Okizuka, Y., Mori, T. *et al.* Molecular characterization of the 5'-UTR of retinal dystrophin reveals a cryptic intron that regulates translational activity. *Mol. Vis.* **16,** 2590–2597 (2010).
26 Roberts, R. G., Barby, T. F., Manners, E., Bobrow, M. & Bentley, D. R. Direct detection of dystrophin gene rearrangements by analysis of dystrophin mRNA in peripheral blood lymphocytes. *Am. J. Hum. Genet.* **49,** 298–310 (1991).
27 Matsuo, M., Masumura, T., Nishio, H., Nakajima, T., Kitoh, Y., Takumi, T. *et al.* Exon skipping during splicing of dystrophin mRNA precursor due to an intraexon deletion in the dystrophin gene of Duchenne muscular dystrophy Kobe. *J. Clin. Invest.* **87,** 2127–2131 (1991).
28 Tran, V. K., Zhang, Z., Yagi, M., Nishiyama, A., Habara, Y., Takeshima, Y. *et al.* A novel cryptic exon identified in the 3' region of intron 2 of the human dystrophin gene. *J. Hum. Genet.* **50,** 425–433 (2005).
29 Bu, D., Yu, K., Sun, S., Xie, C., Skogerbo, G., Miao, R. *et al.* NONCODE v3.0: integrative annotation of long noncoding RNAs. *Nucleic Acids Res.* **40,** D210–D215 (2011).
30 Proudfoot, N. J. Ending the message: poly(A) signals then and now. *Genes Dev.* **25,** 1770–1782 (2012).
31 Cabili, M. N., Trapnell, C., Goff, L., Koziol, M., Tazon-Vega, B., Regev, A. *et al.* Integrative annotation of human large intergenic noncoding RNAs reveals global properties and specific subclasses. *Genes Dev.* **25,** 1915–1927 (2011).
32 Erdmann, V. A., Szymanski, M., Hochberg, A., de Groot, N. & Barciszewski, J. Collection of mRNA-like non-coding RNAs. *Nucleic Acids Res.* **27,** 192–195 (1999).
33 Nagano, T. & Fraser, P. No-nonsense functions for long noncoding RNAs. *Cell* **145,** 178–181 (2011).
34 Bähring, S., Kann, M., Neuenfeld, Y., Gong, M., Chitayat, D., Toka, H. *et al.* Inversion region for hypertension and brachydactyly on chromosome 12p features multiple splicing and noncoding RNA. *Hypertension* **51,** 426–431 (2008).
35 Cao, X., Yeo, G., Muotri, A. R., Kuwabara, T. & Gage, F. H. Noncoding RNAs in the mammalian central nervous system. *Annu. Rev. Neurosci.* **29,** 77–103 (2006).
36 Mercer, T. R., Dinger, M. E., Sunkin, S. M., Mehler, M. F. & Mattick, J. S. Specific expression of long noncoding RNAs in the mouse brain. *Proc. Natl Acad. Sci. USA* **105,** 716–721 (2008).
37 Cesana, M., Cacchiarelli, D., Legnini, I., Santini, T., Sthandier, O., Chinappi, M. *et al.* A long noncoding RNA controls muscle differentiation by functioning as a competing endogenous RNA. *Cell* **147,** 358–369 (2011).

BRIEF REPORT

Human Mutation

OFFICIAL JOURNAL

HGVS HUMAN GENOME VARIATION SOCIETY

www.hgvs.org

Pathogenic Orphan Transduction Created by a Nonreference LINE-1 Retrotransposon

Szilvia Solyom,[1†] Adam D. Ewing,[1,2†] Dustin C. Hancks,[1†] Yasuhiro Takeshima,[3] Hiroyuki Awano,[3] Masafumi Matsuo,[3,4] and Haig H. Kazazian Jr[1*]

[1]*McKusick-Nathans Institute of Genetic Medicine, Johns Hopkins University School of Medicine, Baltimore, Maryland;* [2]*Present address: Center for Biomolecular Science and Engineering, University of California at Santa Cruz, Santa Cruz, California;* [3]*Department of Pediatrics, Graduate School of Medicine, Kobe University, 7-5-1 Kusunokicho, Chuo, Kobe, Japan;* [4]*Present address: Department of Medical Rehabilitation, Faculty of Rehabilitation, Kobegakuin University, Ikawadani-cho, Nishi-ku, Kobe, Japan*

Communicated by Mark H. Paalman

Received 20 September 2011; accepted revised manuscript 10 November 2011.

Published online 17 November 2011 in Wiley Online Library (www.wiley.com/humanmutation).DOI: 10.1002/humu.21663

ABSTRACT: Long INterspersed Element-1 (LINE-1) retrotransposons comprise 17% of the human genome, and move by a potentially mutagenic "copy and paste" mechanism via an RNA intermediate. Recently, the retrotransposition-mediated insertion of a new transcript was described as a novel cause of genetic disease, Duchenne muscular dystrophy, in a Japanese male. The inserted sequence was presumed to derive from a single-copy, noncoding RNA transcribed from chromosome 11q22.3 that retrotransposed into the *dystrophin* gene. Here, we demonstrate that a nonreference full-length LINE-1 is situated in the proband and maternal genome at chromosome 11q22.3, directly upstream of the sequence, whose copy was inserted into the *dystrophin* gene. This LINE-1 is highly active in a cell culture assay. LINE-1 insertions are often associated with 3′ transduction of adjacent genomic sequences. Thus, the likely explanation for the mutagenic insertion is a LINE-1-mediated 3′ transduction with severe 5′ truncation. This is the first example of LINE-1-induced human disease caused by an "orphan" 3′ transduction.

Hum Mutat 33:369–371, 2012. © 2011 Wiley Periodicals, Inc.

KEY WORDS: LINE-1; retrotransposon; 3′ transduction; dystrophin; Duchenne muscular dystrophy

Retrotransposons ("jumping genes") are highly abundant mobile genomic elements. In particular, the long interspersed element-1 (LINE-1 or L1) class comprises 17% of the human genome. A full-length human LINE-1 is about 6 kilobases and contains a 5′ untranslated region (UTR) encoding promoter activity [Swergold, 1990], two open reading frames (ORFs) separated by a spacer [Dombroski et al., 1991], a 3′ UTR, and a poly(A) tail. ORF1 encodes a protein with RNA binding [Hohjoh and Singer, 1996; Martin, 1991] and nucleic acid chaperone activity [Martin and Bushman, 2001], while ORF2 is a protein with endonuclease [Feng et al., 1996] and reverse transcriptase activities [Mathias et al., 1991]. LINE-1s are autonomous nonlong terminal repeat retrotransposons that move by a potentially mutagenic "copy and paste" mechanism via an RNA intermediate that is reverse transcribed and inserted into the genome [reviewed in Goodier and Kazazian, 2008]. LINE-1s can also cause disease indirectly, through mobilization of the nonautonomous Alu and SVA (SIVE-VNTR-Alu) retrotransposons [Dewannieux et al., 2003; Hancks et al., 2011; Ostertag et al., 2003].

Recently, the retrotransposition-mediated insertion of a new cDNA was described as a novel cause of genetic disease, Duchenne muscular dystrophy (MIM# 310200), in a Japanese boy [Awano et al., 2010]. In this work, it was presumed that the inserted sequence was derived from a nonrepetitive noncoding RNA transcribed from chromosome 11q22.3 that was reverse transcribed and integrated in the antisense orientation into exon 67 of the *dystrophin* gene on chromosome X, causing exon 67 skipping. The whole insertion was 327-bp long, of which 212 bp was identical to a sequence on chromosome 11q22.3 (chr11:105,479,198–105,479,409 of hg19/NCBI Build 37.1 Feb 2009), while the remaining 115 bp was a poly(T) stretch. The inserted sequence had hallmarks of LINE-1 retrotransposition, namely a poly(A) tail complementary to the poly(T) stretch, target site duplication flanking the insertion in *dystrophin* exon 67, and insertion at a near-consensus LINE-1 endonuclease site (TTTT/CA instead of TTTT/AA) [Awano et al., 2010]. Another LINE-1-related phenomenon is 3′ transduction, the co-mobilization of DNA sequences downstream of LINE-1s as a consequence of transcriptional read-through due to the weak LINE-1 poly(A) signal [Holmes et al., 1994; Moran et al., 1996]. Because LINE-1 insertions are often associated with 3′ transductions [Goodier et al., 2000; Moran et al., 1999; Pickeral et al., 2000], we hypothesized that the insertion in the patient might result from such an event. However, no LINE-1 was present in the DNA upstream of the single copy sequence from chromosome 11q22.3 in the human reference genome (hg19).

On the other hand, a LINE-1 directly upstream of the transduced sequence on chromosome 11q22.3 was present in one Japanese individual of 15 unrelated individuals in a LINE-1-targeted resequencing dataset generated in our laboratory [Ewing and Kazazian, 2010]. Based on bioinformatic analysis, this LINE-1 was absent from the 185 HapMap phase I individuals, including 30 individuals with self-reported Japanese ancestry, whose genomes were sequenced by the 1000 Genomes Consortium [1000 Genomes

†These authors contributed equally to this work and should be considered joint first authors.

*Correspondence to: Haig H. Kazazian Jr, Johns Hopkins University School of Medicine, Broadway Research Building, Room 439, 733 N. Broadway, Baltimore, MD 21205. E-mail: kazazian@jhmi.edu

Contract grant sponsor: NIH (RC4MH092880 to H.H.K).

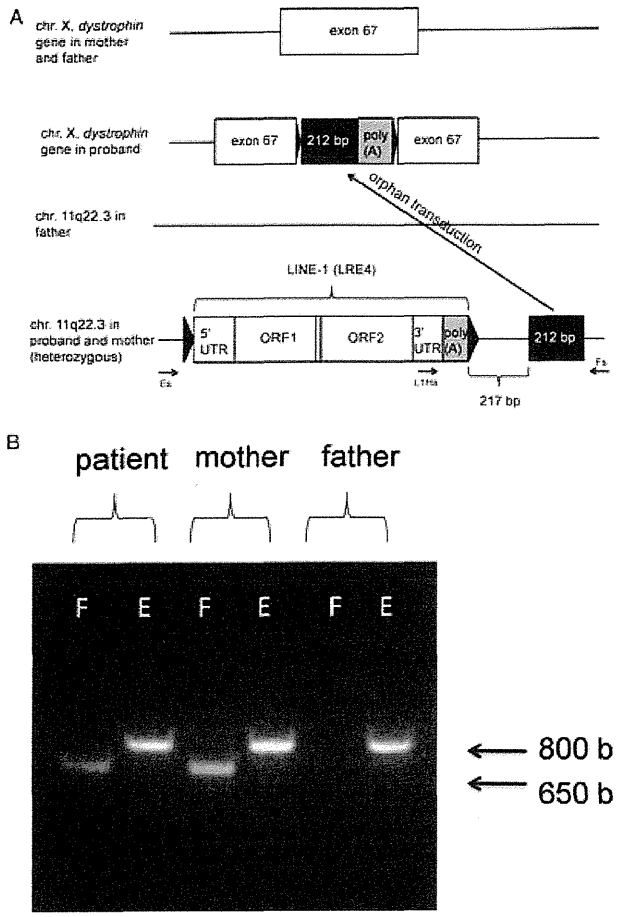

Figure 1. **A:** Orphan 3′ transduction event in the patient. The transduced sequence is in black. Black triangles indicate target site duplications (3 bp in exon 67, 21 bp at chromosome 11q22.3). **B:** PCR analysis of the 3′ junctions of the presumed progenitor (LRE4) of the DNA sequence inserted into the *dystrophin* gene with the primers indicated in A. Genotyping primer pairs L1Hs (5′-GGGAGATATACCTAATGCTAGATGACAC-3′) and Fs (5′-CGTTACATTTCACCACAGATTG-3′) amplify the filled (F) site (around 686 bp), while primers Es (5′-AGCACAATACCTTGCACATTAG-3′) and Fs amplify only the empty (E) site (828 bp) due to short primer extension time. Forty Japanese individuals (80 chromosome 11s) were also genotyped for the LRE4 allele and five were positive (data not shown). Thus, this allele is an uncommon variant in the Japanese population. PCR conditions are available upon request.

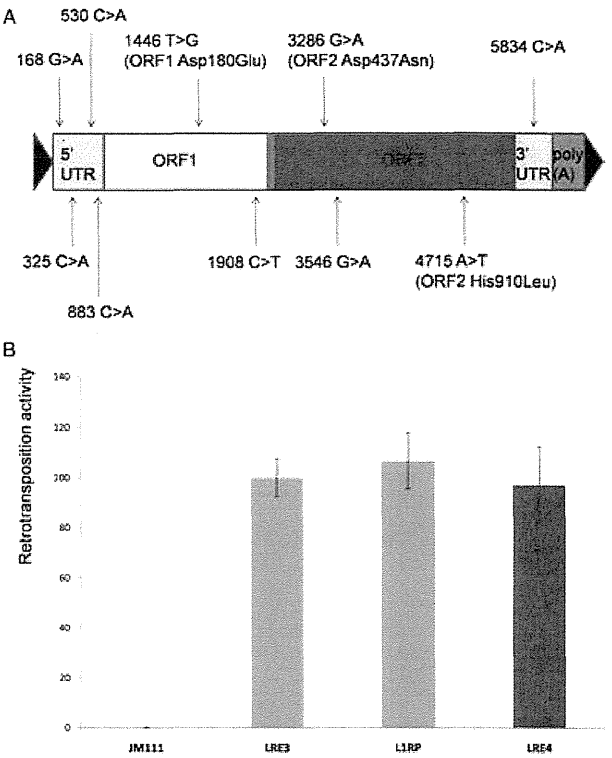

Figure 2. **A:** Schematic diagram of LRE4. Nucleotide changes differing from LRE3 [Brouha et al., 2002] are indicated. LRE4 was PCR amplified from the patient's blood DNA with iProof High Fidelity DNA Polymerase (Bio-Rad, Hercules, CA) and sequenced. LRE4 belongs to the Ta-1d class of human-specific LINE-1s [Boissinot et al., 2000], and the Ta class elements cause most de novo pathogenic human insertions [reviewed in Chen et al., 2005]. **B:** Retrotransposition activity of LRE4 (99-LRE4-EGFP-Puro) in HEK293T cells. LRE4 was PCR amplified with iProof High-Fidelity DNA Polymerase (Bio-Rad) using the primers 5′-CGTTACATTTCACCACAGATTG-3′ and 5′-AAGTAAAATAGAGGTTTTGGGGG-3′. The PCR product was cloned with the TOPO XL PCR Cloning Kit (Invitrogen, Carlsbad, CA) and was subsequently cloned to replace L1RP in the 99-RPS-EGFP-Puro reporter construct with *Bst*Z17I and *Not*I-HF double digestion and ligation. HEK293T cells were transfected with 1 μg of each plasmid in a 6-well plate using Fugene 6 (Roche, Indianapolis, IN). Transfected cells were selected with puromycin, and retrotransposition events were evaluated 4 days later by FACS analysis of EGFP expressing cells. 99-RPS is the highly active L1RP cloned into a modified pCEP4 plasmid lacking the CMV promoter. Retrotransposition activity of 99-LRE3-EGFP-Puro is set to 100%. JM111 has the same sequence as 99-RPS, except that it contains two point mutations in ORF1 that abolish retrotransposition in cis [Moran et al., 1996] and serves as a negative control. Retrotransposition activity of L1RP and LRE3 was similar in HEK293T cells. Standard deviation of two independent experiments done in triplicate is shown.

Project Consortium, 2010; Stewart et al., 2011]. Additionally, it was not detected in our independent whole-genome analysis of individuals included in the 1000 Genomes project [Ewing and Kazazian, 2011]. The lack of evidence for this insertion in multiple analyses indicates that it may represent a population-restricted variant present at low allele frequency in the general population. To evaluate further its gene frequency in the Japanese population, we analyzed 80 Japanese chromosome 11q22.3 sites by PCR and found five sites containing the LINE-1, corresponding to a gene frequency of 6% (data not shown). Here, we demonstrate through PCR-based analysis that this nonreference LINE-1 is full length and is situated in the maternal and proband genomes at chromosome 11q22.3, 217 bp 5′ of the retrotransposed 212-bp sequence that was inserted into the *dystrophin* gene (Fig. 1A and B). Thus, the most likely explanation for the mutagenic insertion is a LINE-1-induced 3′ transduction event from chromosome 11q22.3 with severe 5′ truncation upon insertion, such that only part of the 3′ transduced sequence was inserted (Fig. 1A). What is less clear is in which cell lineage and at what time-point the LINE-1 RNA was reverse transcribed and inserted into the genome. Integration into the *dystrophin* gene most likely occurred in one or more of the mother's germ cells or early during the proband's development, because the mother's blood was negative for the presence of the 3′ transduced sequence.

To characterize the LINE-1 progenitor element on chromosome 11q22.3, hereafter referred to as LRE4 (LINE-1 Retrotransposable Element 4; BankIt1482137 LRE4 JN698885 [GenBank, http://www.ncbi.nlm.nih.gov/Genbank/]), we PCR amplified it

from the patient's blood DNA and sequenced it from multiple independent PCR products, all of which had the identical sequence. LRE4 is a full length Ta-1d element and contains 10 nucleotide alterations relative to LRE3, the most active LINE-1 isolated to date, and the only LINE-1 that is an exact match to the active LINE-1 amino acid consensus sequence [Brouha et al., 2002, 2003]. Three of the nucleotide substitutions in LRE4 resulted in amino acid changes relative to LRE3 (Fig. 2A). All LRE4 nucleotide changes were identified in other LINE-1s present in the hg19 assembly. However, no reference LINE-1 contained all 10 nucleotide alterations, nor was it present in a recent dataset of active LINE-1s [Beck et al., 2010]. To determine the retrotransposition activity of LRE4, we cloned it into a plasmid with an enhanced green fluorescent protein (EGFP) retrotransposition indicator cassette, creating 99-LRE4-EGFP-Puro. This cassette was designed so that translation of the EGFP reporter gene occurs only after LINE-1 reverse transcription and integration of its cDNA copy into the genome—that is, after a retrotransposition event [Moran et al., 1996; Ostertag et al., 2000]. Upon transfection of HEK293T cells with 99-LRE4-EGFP-Puro, and selection for transfected cells with puromycin, retrotransposition events were evaluated by FACS analysis of EGFP expressing cells [Ostertag et al., 2000]. 99-LRE4-EGFP-Puro demonstrated a retrotransposition activity comparable to plasmids containing LRE3 or L1RP (Fig. 2B), indicating that it is a highly active or "hot" retrotransposon [Brouha et al., 2003].

This is the fifth case of LINE-1-driven insertional mutagenesis of the *dystrophin* gene [Narita et al., 1993; Yoshida et al., 1998; Musova et al., 2006; and Awano et al., 2010 together with the current study]. Therefore, mutation analyses of this gene should take into account large insertions mediated by LINE-1s. Although, LINE-1s are often truncated at their 5′ end, this is the first example of LINE-1-induced human disease caused by an orphan 3′ transduction, that is, a LINE-1-mediated insertion lacking LINE-1 sequence. Two nondisease causing retrotransposition events of gene fragments have also been described that may have arisen by LINE-1-mediated 3′ transduction, with the transducing LINE-1 being lost [Ejima and Yang, 2003; Rozmahel et al., 1997]. In a previous report, we showed that a mutagenic insertion into the *α-spectrin* gene was the result of an SVA-mediated orphan 3′ transduction [Ostertag et al., 2003]. Therefore, any insertion of a nonrepetitive sequence bearing the hallmarks of retrotransposition should be further investigated for a LINE-1- or SVA-mediated transduction event, as previously postulated by Moran et al. [1999]. Our results indicate that LRE4 is a highly active, polymorphic retrotransposon with a pathogenic history.

Acknowledgments

We thank John L. Goodier and Prabhat K. Mandal for their great insights into the project and for their comments on the manuscript. Ling Cheung and David Sigmon are acknowledged for excellent technical assistance. We thank Dr. Christine Beck and Dr. John Moran for sharing their data concerning hot LINE-1s.

Disclosure Statement: The authors declare no conflict of interest.

References

Awano H, Malueka RG, Yagi M, Okizuka Y, Takeshima Y, Matsuo M. 2010. Contemporary retrotransposition of a novel non-coding gene induces exon-skipping in dystrophin mRNA. J Hum Genet 55:785–790.

Beck CR, Collier P, Macfarlane C, Malig M, Kidd JM, Eichler EE, Badge RM, Moran JV. 2010. LINE-1 retrotransposition activity in human genomes. Cell 141:1159–1170.

Boissinot S, Chevret P, Furano AV. 2000. L1 (LINE-1) retrotransposon evolution and amplification in recent human history. Mol Biol Evol 17:915–928.

Brouha B, Meischl C, Ostertag E, de Boer M, Zhang Y, Neijens H, Roos D, Kazazian HH, Jr. 2002. Evidence consistent with human L1 retrotransposition in maternal meiosis I. Am J Hum Genet 71:327–336.

Brouha B, Schustak J, Badge RM, Lutz-Prigge S, Farley AH, Moran JV, Kazazian HH, Jr. 2003. Hot L1s account for the bulk of retrotransposition in the human population. Proc Natl Acad Sci USA 100:5280–5285.

Chen JM, Stenson PD, Cooper DN, Ferec C. 2005. A systematic analysis of LINE-1 endonuclease-dependent retrotranspositional events causing human genetic disease. Hum Genet 117:411–427.

Dewannieux M, Esnault C, Heidmann T. 2003. LINE-mediated retrotransposition of marked Alu sequences. Nat Genet 35:41–48.

Dombroski BA, Mathias SL, Nanthakumar E, Scott AF, Kazazian HH, Jr. 1991. Isolation of an active human transposable element. Science 254:1805–1808.

Ejima Y, Yang L. 2003. Trans mobilization of genomic DNA as a mechanism for retrotransposon-mediated exon shuffling. Hum Mol Genet 12:1321–1328.

Ewing AD, Kazazian HH, Jr. 2010. High-throughput sequencing reveals extensive variation in human-specific L1 content in individual human genomes. Genome Res 20:1262–1270.

Ewing AD, Kazazian HH, Jr. 2011. Whole-genome resequencing allows detection of many rare LINE-1 insertion alleles in humans. Genome Res 21:985–990.

Feng Q, Moran JV, Kazazian HH, Jr, Boeke JD. 1996. Human L1 retrotransposon encodes a conserved endonuclease required for retrotransposition. Cell 87:905–916.

1000 Genomes Project Consortium. 2010. A map of human genome variation from population-scale sequencing. Nature 467:1061–1073.

Goodier JL, Kazazian HH, Jr. 2008. Retrotransposons revisited: the restraint and rehabilitation of parasites. Cell 135:23–35.

Goodier JL, Ostertag EM, Kazazian HH, Jr. 2000. Transduction of 3′-flanking sequences is common in L1 retrotransposition. Hum Mol Genet 9:653–657.

Hancks DC, Goodier JL, Mandal PK, Cheung LE, Kazazian HH, Jr. 2011. Retrotransposition of marked SVA elements by human L1s in cultured cells. Hum Mol Genet 20:3386–3400.

Hohjoh H, Singer MF. 1996. Cytoplasmic ribonucleoprotein complexes containing human LINE-1 protein and RNA. EMBO J 15:630–639.

Holmes SE, Dombroski BA, Krebs CM, Boehm CD, Kazazian HH, Jr. 1994. A new retrotransposable human L1 element from the LRE2 locus on chromosome 1q produces a chimaeric insertion. Nat Genet 7:143–148.

Martin SL. 1991. Ribonucleoprotein particles with LINE-1 RNA in mouse embryonal carcinoma cells. Mol Cell Biol 11:4804–4807.

Martin SL, Bushman FD. 2001. Nucleic acid chaperone activity of the ORF1 protein from the mouse LINE-1 retrotransposon. Mol Cell Biol 21:467–475.

Mathias SL, Scott AF, Kazazian HH, Jr, Boeke JD, Gabriel A. 1991. Reverse transcriptase encoded by a human transposable element. Science 254:1808–1810.

Moran JV, DeBerardinis RJ, Kazazian HH, Jr. 1999. Exon shuffling by L1 retrotransposition. Science 283:1530–1534.

Moran JV, Holmes SE, Naas TP, DeBerardinis RJ, Boeke JD, Kazazian HH, Jr. 1996. High frequency retrotransposition in cultured mammalian cells. Cell 87:917–927.

Musova Z, Hedvicakova P, Mohrmann M, Tesarova M, Krepelova A, Zeman J, Sedlacek Z. 2006. A novel insertion of a rearranged L1 element in exon 44 of the dystrophin gene: further evidence for possible bias in retroposon integration. Biochem Biophys Res Commun 347:145–149.

Narita N, Nishio H, Kitoh Y, Ishikawa Y, Ishikawa Y, Minami R, Nakamura H, Matsuo M. 1993. Insertion of a 5′ truncated L1 element into the 3′ end of exon 44 of the dystrophin gene resulted in skipping of the exon during splicing in a case of Duchenne muscular dystrophy. J Clin Invest 91:1862–1867.

Ostertag EM, Goodier JL, Zhang Y, Kazazian HH,Jr. 2003. SVA elements are nonautonomous retrotransposons that cause disease in humans. Am J Hum Genet 73:1444–1451.

Ostertag EM, Prak ET, DeBerardinis RJ, Moran JV, Kazazian HH,Jr. 2000. Determination of L1 retrotransposition kinetics in cultured cells. Nucleic Acids Res 28:1418–1423.

Pickeral OK, Makalowski W, Boguski MS, Boeke JD. 2000. Frequent human genomic DNA transduction driven by LINE-1 retrotransposition. Genome Res 10:411–415.

Rozmahel R, Heng HH, Duncan AM, Shi XM, Rommens JM, Tsui LC. 1997. Amplification of CFTR exon 9 sequences to multiple locations in the human genome. Genomics 45:554–561.

Stewart C, Kural D, Stromberg MP, Walker JA, Konkel MK, Stutz AM, Urban AE, Grubert F, Lam HY, Lee WP, Busby M, Indap AR, Garrison E, Huff C, Xing J, Snyder MP, Jorde LB, Batzer MA, Korbel JO, Marth GT, 1000 Genomes Project. 2011. A comprehensive map of mobile element insertion polymorphisms in humans. PLoS Genet 7:e1002236.

Swergold GD. 1990. Identification, characterization, and cell specificity of a human LINE-1 promoter. Mol Cell Biol 10:6718–6729.

Yoshida K, Nakamura A, Yazaki M, Ikeda S, Takeda S. 1998. Insertional mutation by transposable element, L1, in the DMD gene results in X-linked dilated cardiomyopathy. Hum Mol Genet 7:1129–1132.

GTMB-2010-0276-ver9-Ota_1P
Type: research-article

GENETIC TESTING AND MOLECULAR BIOMARKERS
Volume 00, Number 00, 2011

Pp. 1–6
DOI: 10.1089/gtmb.2010.0276

ORIGINAL ARTICLE

AU1 ▶

A G-to-T Transversion at the Splice Acceptor Site of Dystrophin Exon 14 Shows Multiple Splicing Outcomes That Are Not Exemplified by Transition Mutations

Mitsunori Ota, Yasuhiro Takeshima, Atsushi Nishida, Hiroyuki Awano, Tomoko Lee, Mariko Yagi, and Masafumi Matsuo

Mutations at splicing consensus sequences have been shown to induce splicing errors such as exon skipping or cryptic splice site activation. Here, we identified eight splicing products caused by a G-to-T transversion mutation at the splice acceptor site of exon 14 of the dystrophin gene (c.1603–1G>T). Unexpectedly, the most abundant product showed skipping of the two consecutive exons 14 and 15, and exon 14 skipping was observed as the second most abundant product. To examine the cause of this splicing multiplicity, minigenes containing dystrophin exons 14 and 15 with their flanking introns were constructed and subjected to *in vitro* splicing. Minigenes with the wild-type sequence or a G>A transition at position c.1603–1 produced only the mature mRNA. On the other hand, the minigenes with a G>T or G>C transversion mutation produced multiple splicing products. A time-course analysis of the *in vitro* splicing revealed that splicing of the middle intron, intron 14, was the first step in transcript maturation for all four minigene constructs. The identity of the mutant nucleotide, but not its position, is a factor leading to multiple splicing outcomes. Our results suggest that exon skipping therapy for Duchenne's muscular dystrophy should be carefully monitored for their splicing outcomes.

Introduction

Splicing is a highly regulated process that removes intron sequences from pre-mRNA. The process proceeds from the 5′ to the 3′ end of the pre-mRNA to assemble the ordered array of exons in mature transcripts (Keren *et al.*, 2010; Licatalosi and Darnell, 2010). Splicing depends on the correct identification of exons, which must be recognized within the pre-mRNA despite being relatively short compared with introns. It is known that the presence of well-defined cis-elements, namely the splice donor and acceptor sites and the branch point, are necessary but not sufficient to define intron–exon boundaries (Senapathy *et al.*, 1990). A critical step in pre-mRNA splicing is the recognition and pairing of splice donor and acceptor sites, where GT and AG dinucleotides are strictly conserved sequences, respectively. Mutations at these consensus sequences result in splicing errors such as exon skipping and cryptic splice site activation and are responsible for nearly 15% of all genetic diseases (Hertel, 2008).

Duchenne's and Becker muscular dystrophy (DMD/BMD) are the most common forms of inherited myopathy and are caused by mutations in the dystrophin gene. DMD is a rapidly progressive disease that usually results in the death of patients in their twenties, whereas BMD is a clinically less severe form of the disease and often has only a slightly debilitating effect. The difference between DMD and BMD can be explained by the reading frame rule: frame-shift mutations that generate premature stop codons in the coding sequence of dystrophin mRNA usually result in the DMD phenotype, whereas mutations that maintain the original reading frame cause the milder BMD phenotype (Monaco *et al.*, 1988). Therefore, it is important to consider how splice site mutations could alter the splicing products of the dystrophin gene, and thus whether they will lead to either the DMD or the BMD phenotype. For this reason, dystrophinopathy is one of the most extensively studied diseases related to splice site mutations and their resultant products (Matsuo *et al.*, 1991; Nishiyama *et al.*, 2008).

The dystrophin gene is the largest human gene, spanning 2500 kb on the X chromosome. It has a complex structure, including a large number of exons, long introns, and several alternative promoters (Den Dunnen *et al.*, 1989; Ahn and Kunkel, 1993; Nishio *et al.*, 1994). Dystrophin pre-mRNA splicing would seem to require extraordinarily strict regulation. However, single-nucleotide mutations in splice acceptor or donor sites have been reported to cause splicing alterations, including exon skipping, cryptic splice site activation, or both (Hagiwara *et al.*, 1994; Tuffery-Giraud *et al.*, 1999; Adachi *et al.*,

Department of Pediatrics, Graduate School of Medicine, Kobe University, Kobe, Japan.

2003; Thi Tran *et al.*, 2005; Habara *et al.*, 2009). Despite the identification of a large number of splice site mutations in many diseases, there is still no established way to predict what splicing patterns these mutations will produce (Wimmer *et al.*, 2007; Hertel, 2008).

In this study, we identified multiple splicing outcomes caused by a transversion mutation at the splice acceptor site of dystrophin exon 14. In *in vitro* splicing assays, transversion but not transition mutations induced multiple splicing outcomes. We suggest that the manipulation of splicing with antisense oligonucleotides (AOs) should be carefully evaluated in DMD treatment.

Materials and Methods

Genomic DNA analysis

Genomic DNA was extracted from a BMD male (KUCG557) and a control as previously described (Matsuo *et al.*, 1990). A mutation in the dystrophin gene was sought by direct sequencing (Nishiyama *et al.*, 2008; Takeshima *et al.*, 2010).

Dystrophin mRNA analysis

Dystrophin mRNA in skeletal muscle was analyzed as previously described (Roberts *et al.*, 1991; Surono *et al.*, 1999). A fragment spanning exons 13 to 18 was amplified by reverse transcription–polymerase chain reaction (RT-PCR) using a set of primers (c13f; 5′-GCTGCTTTGGAAGAACAACTT-3′ and 1F; 5′-CTTCTGAGCGAGTAATCCAGCT-3′) using conditions as previously described (Habara *et al.*, 2009). The amplified products were sequenced after subcloning, as previously described (Thi Tran *et al.*, 2005).

In vitro *splicing analysis*

In vitro splicing analysis was conducted using the preconstructed minigene of the expression vector H492 that encodes two cassette exons (exons A and B) and a multicloning site in the intervening sequence (Habara *et al.*, 2008).

A region spanning intron 13, exon 14, intron 14, exon 15, and intron 15 was PCR amplified from genomic DNA of the index case and a control using the primer set: 5′-GCGG CTAGCTCAGAAAGAGTGTCCCTTCCAA-3′ and 5′-GCGG GATCCCACTTTAATTCAGAAAAGTAGCAA-3′. Amplified products were digested with *Nhe*I and *Bam*HI restriction enzymes (New England Biolabs, Ipswich, MA) and inserted into the H492 vector that was predigested with the same enzymes. Two mutant constructs, c.1603–1G>A and c.1603–1G>C, were prepared by means of overlap extension PCR and were inserted into the H492 vector. After checking their sequences, the resultant plasmids were transfected into HeLa cells for splicing assays as previously described (Habara *et al.*, 2009). The cells were harvested after 24 h of incubation for extraction of total RNA.

Time-course analysis

To determine the splicing order of the introns, *in vitro* splicing was stopped after 1, 2, 3, or 4 h by extracting total RNA. The resulting splicing products were analyzed as previously described. RT-PCR products were semiquantified using a DNA 1000 LabChip kit on an Agilent 2100 Bioanalyzer (Agilent Technologies, Santa Clara, CA) and their sequences were determined by subcloning and sequencing.

Results

A G-to-T transversion mutation was identified at the 3′ end of intron 13 of the dystrophin gene (c.1603–1G>T) in a Japanese BMD patient (Fig. 1). Although the mutation was located within an intron, the mutation changed the highly conserved AG dinucleotides at the splice acceptor site to AT, thereby decreasing the splice site strength (Ri) of the splice acceptor site from 12.3 to 3.5. It was strongly expected that skipping of the downstream exon 14 would be the splicing outcome of this mutation. However, dystrophin mRNA expressed in the patient's skeletal muscle was found to contain multiple splicing products. When a region spanning exons 13 to 18 was amplified by RT-PCR, four amplified bands were visualized

◀ F1

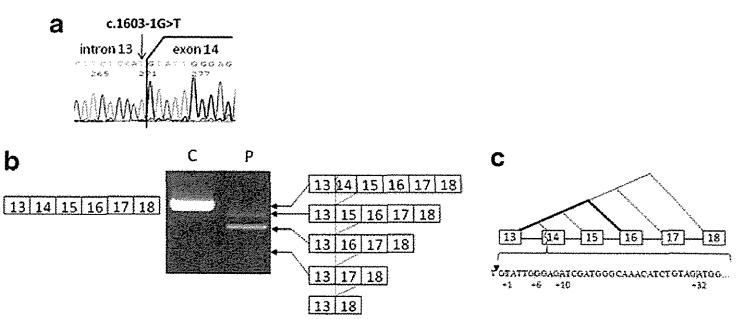

FIG. 1. Genomic and mRNA analysis of the dystrophin gene. **(a)** Sequence of the intron 13/exon 14 junction. A genomic PCR product from the index case (KUCG557), a Becker muscular dystrophy patient, was directly sequenced. The terminal nucleotide of intron 13 (c.1603–1) was identified to be T, indicating a G-to-T transversion mutation (c.1603–1G>T; indicated by the arrow). **(b)** RT-PCR products encompassing exons 13 to 18. Amplified products obtained from the control (C) and patient (P) are shown. The identity of the bands is indicated on either side of the gel image. Boxes and numbers within the boxes indicate exons and exon numbers, respectively. The vertical wavy line indicates activated cryptic splice sites. **(c)** Schematic of potential splicing patterns. The approximate frequency of each identified splicing pattern is distinguished by the lines joining the boxes (bold line, high frequency; dashed line, low frequency; regular line, intermediate frequency). Details of cryptic splice sites detected around the 5′ end of exon 14 are shown as a magnified image (bottom). Four vertical dashed lines located at nucleotides +1, +6, +10, and +32 within exon 14 indicate cryptic splice sites that were activated by the mutation. The inverted triangle indicates the junction between intron 13 and exon 14. RT-PCR, reverse transcription–polymerase chain reaction.

on agarose gels, with different densities from clearly visible to barely visible (Fig. 1). Unexpectedly, subcloning and sequencing revealed that the most abundant product lacked not only exon 14 but also exon 15, indicating the skipping of two consecutive exons (Fig. 1). The second most abundant product corresponded to the expected product that lacked only exon 14. As these two abundant mRNAs maintained the original dystrophin reading frame, the index case was diagnosed as BMD at the mRNA level. This matched with his clinical phenotype.

The third faintly visible product, which corresponded to the wild-type dystrophin size, maintained all six exons from exons 13 to 18. However, subcloning and sequencing of this band revealed four different clones, containing a deletion of 1, 6, 10, or 32 nucleotides at the 5′ end of exon 14 (Fig. 1). It was unclear whether these were genuine splicing products or artifacts. Examination of the genomic sequences around these unexpected deletions revealed that the ends of two of the deletions, at the 10th and 32nd nucleotides, comprise AG dinucleotides, whereas the ends of the other two, at the 1st and 6th nucleotides, comprise TG dinucleotides (Fig. 1). Because all these four sites scored as potential splice acceptor sites, it was concluded that all four clones were derived from alternative splicing products, activating a cryptic splice acceptor site located +1, +6, +10, or +32 nucleotides from the intron 13/exon 14 boundary (Fig. 1). The smallest, barely visible band lacked exons 14, 15, and 16 (Fig. 1) and clones lacking exons 14, 15, 16, and 17 were also identified. Eight splicing patterns had been identified in the patient's muscle RNA: four patterns of exon skipping and four patterns of cryptic splice site activation (Fig. 1).

Multiple splicing outcomes caused by a single-nucleotide change at the splice acceptor site of the mammoth dystrophin gene were unexpected. This suggested that the mutation identified in the index case exerts a strong influence on the splicing machinery. To demonstrate this, an *in vitro* splicing system using the H492 minigene was employed. Fragments encompassing exons 14–15 and their flanking introns, with wild-type or mutant (c.1603–1G > T) sequence, were amplified from genomic DNA by PCR and inserted into the multicloning site within the intron between exons A and B of the H492 minigene (Fig. 2a). Constructed minigenes were transfected into HeLa cells and the resulting splicing products were analyzed by RT-PCR after 24 h. From the wild-type construct, a single amplified product was obtained and was confirmed to be the expected mature mRNA consisting of exons A, 14, 15, and B (Fig. 2). This *in vitro* system was therefore confirmed to effect accurate splicing of dystrophin exons 14 and 15.

F2 ▶

For the mutant minigene harboring the c.1603–1G > T transversion, multiple RT-PCR amplification products were identified: one major band, two minor bands, and one weak band (Fig. 2). Sequencing of the major band revealed an intermediate splicing product that lacked both introns 14 and 15 but retained intron A unspliced. This indicated that the splicing machinery recognized the two downstream introns, but not the upstream intron A in the presence of the c.1603–1G > T change. This outcome was compatible with the disruption of the splice acceptor site of intron A by the mutation. By subcloning and sequencing of the two minor products and the one weak product, four clones were identified, which differed in their exon 14 5′ end sequences in the mature mRNA. Each had a 1-, 4-, 10-, or 32-nucleotide deletion from the 5′ end

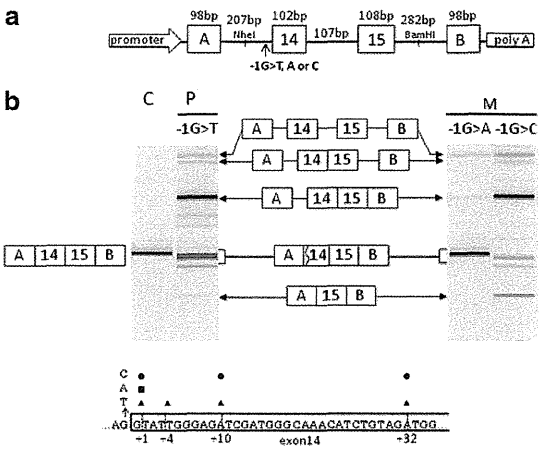

FIG. 2. *In vitro* splicing analysis. **(a)** Schematic showing the structure of the minigenes. The genomic regions spanning dystrophin exons 14, 15, and their respective adjacent introns, containing wild-type or mutant (c.1603–1G > T, G > A, or G > C) sequence, were inserted into the *Nhe*I and *Bam*HI sites between exons A and B in the H492 vector. Boxes and lines indicate exons and introns, respectively. At the 5′ and 3′ end, respectively, there is a promoter and poly(A) addition signal. The lengths of the exons and introns are indicated. **(b)** RT-PCR products of minigene transcripts. Capillary gel electrophoresis patterns of RT-PCR-amplified products from the minigenes carrying the wild-type (c.1603–1G) (C) or the mutant (c.1603–1G > T or G > C) (M) sequence are shown. The identity of the splicing products is indicated on either side. Boxes and numbers within the boxes indicate exons and exon numbers, respectively. The vertical wavy line indicates the position of the cryptic splice sites. Details of the cryptic splice sites (vertical dashed lines) detected around the 5′ end of exon 14 are shown as a magnified image (bottom). The numbers indicate the nucleotide number within exon 14. The activated cryptic splice sites are marked by black triangles, black squares, and black circles in the minigenes with c.1603–1G > T, G > A, and G > C, respectively.

of exon 14 (Fig. 2); the 10-bp deletion was the most common. Although activation of four cryptic splice acceptor sites within exon 14 was shown *in vitro* as well as *in vivo*, only three were common to both. *In vivo*, the sixth nucleotide was activated as a cryptic splice site (TG), whereas *in vitro*, the 4th nucleotide was activated (AT). Remarkably, pre-mRNAs maintaining all three introns and mRNA lacking only intron 14 were identified. Because the pre-mRNA was not detected for the wild-type minigene, the G > T mutation was considered to affect the splicing reaction fundamentally. However, skipping of exons 14 and 15, or the single exon 14, was not observed *in vitro*. It was unclear why the expected exon skipping did not occur, even though multiple splicing outcomes caused by the G > T transversion mutation were exemplified *in vitro* (Fig. 2).

We questioned whether nucleotide changes other than the G > T transversion located at an identical position would also produce multiple splicing outcomes. Minigenes with substitution of G to A or C were constructed and subjected to the same *in vitro* splicing assays. Unexpectedly, the minigene with the G > A transition mutation produced one clear band

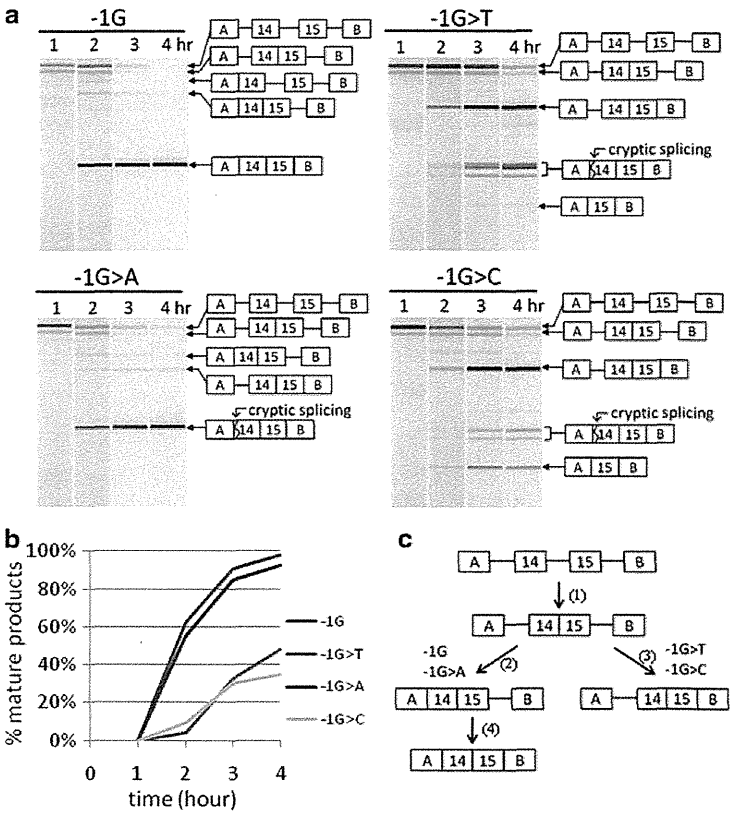

FIG. 3. Time-course analysis of minigene splicing reactions. **(a)** Capillary electrophoresis patterns of RT-PCR products from minigenes with G, T, A, or C at position c.1603–1 are shown. The identity of the splicing products is indicated on the right-hand side. **(b)** The percentage of mature mRNA among all RT-PCR products is shown according to the reaction time. Mature mRNA identified at each time point was expressed as the percentage of the total amplified product. Mature mRNA rapidly increased and, after 4 h, constituted >90% of the total for the wild-type and G>A mutant minigenes. In contrast, at the same time point, mature mRNA constituted less than half of the total for the mutant minigenes with transversion mutations (G>T or G>C). **(c)** Schematic showing the main splicing pathways of the minigene transcripts. For all four minigenes, splicing of intron 14 occurred first (1), producing a splicing intermediate. For the wild-type minigene or the G>A transition mutant, the splicing of intron A then proceeded, producing another intermediate (2), whereas for the G>T or G>C construct, splicing of intron 15 occurs, producing another intermediate (3). Finally, splicing of intron 15 proceeds to produce mature mRNA in the wild-type or G>A mutant minigene (4).

(Fig. 2). Interestingly, this product corresponded to the mature mRNA but had a deletion of a G nucleotide at the 5′ end of exon 14. This G nucleotide was probably recognized as the last nucleotide of intron A, resulting in a simple splicing outcome. This minigene also produced a faint band corresponding to pre-mRNA; this was probably due to disturbance of the entire splicing reaction (Fig. 2).

Remarkably, the minigene with the G>C transversion mutation produced many products: one major band, four additional weak bands, and one barely discernible band. The most abundant band corresponded to a splicing intermediate that removed two downstream introns (introns 14 and 15) but retained intron A (Fig. 2). The second abundant, smallest product had the exon structure A–15–B, indicating exon 14 skipping. In addition, three transcripts were identified with 1-, 10-, or 32-nucleotide deletions at the 5′ end of exon 14 of the mature mRNA (Fig. 2), indicating three cryptic splice site activations. The G>C transversion mutation induced multiple splicing outcomes. These results indicated that a single-nucleotide change at the splice acceptor site changed the splicing pathways, but the splicing outcomes *per se* were dependent on the particular substituted nucleotide.

To clarify the splicing process in transversion or transition mutations at c.1603–1, the time course of the splicing reactions in the minigenes was investigated 1–4 h after transfection. After 1 h, an intermediate product that lacked intron 14 was detected for all four minigenes, in addition to the pre-mRNA (Fig. 3). This indicated that the first step of splicing occurs at the middle intron (intron 14), even in the presence of a normal splice acceptor site for intron A. After 2 h, the mature mRNA constituted >60% of the total mRNA for the wild-type minigene and 55% for the G>A mutant minigene, indicating an uneventful splicing reaction. In contrast, mature mRNA constituted only 10%–20% for minigenes with the G>T or G>C transversions. This indicated that splicing of intron A in the context of a G>T or G>C transversion was strongly inhibited. After 3 h, >80% of the total transcripts were mature mRNA for the wild-type minigene or for the minigene with the G>A transition. However, mature mRNA with activated cryptic splice sites within intron A occupied <40% for the minigenes with the G>T or G>C transversion. This indicated that the last step, the splicing of intron A, was strongly hampered in the presence of a transversion mutation. ◀F3

After 4 h, the splicing reaction was almost complete, with mature mRNA constituting >90% of the total transcripts for the wild-type minigene or the minigene with the G>A mutation. For minigenes with the G>T or G>C transversion, mature mRNA comprised less than half of the total. We considered this to be due to severe disturbance of the splicing of intron A in the presence of a transversion mutation.

In summary, we found that transversion mutations led to multiple splicing outcomes by suppressing splicing reactions. Our data suggest that the identity of the mutant nucleotide can dramatically influence splicing outcome.

Discussion

In this study, a transversion mutation from G to T (c.1603–1G > T) at the splice acceptor site of exon 14 of the dystrophin gene was shown to induce multiple splicing outcomes in a Japanese BMD case. Altogether, eight splicing patterns for dystrophin mRNA were identified in the patient's muscle (Fig. 1). We questioned why this wide variety of splicing patterns was produced from a single-nucleotide change.

In the dystrophin gene, 80 donor and 137 acceptor splice site mutations have been reported (www.dmd.nl/nmdb/home.php). Most of these showed skipping of an adjacent exon as the outcome of the mutation, and some resulted in cryptic splice site activation (Bartolo *et al.*, 1996; Adachi *et al.*, 2003; Thi Tran *et al.*, 2005). Skipping of multiple exons has been reported only rarely: among the reported splice site mutations of the dystrophin gene, only six have been described to induce skipping of multiple exons (Tuffery-Giraud *et al.*, 2004, 2005; Deburgrave *et al.*, 2007; Taylor *et al.*, 2007; Takeshima *et al.*, 2010). Of these six, three were splice acceptor site mutations including the present case. Three were splice donor site mutations, but two of these were an identical mutation at the splice donor site of exon 29 (Deburgrave *et al.*, 2007). It was supposed that splice acceptor site mutations have a greater tendency to promote multiple exon skipping. It is remarkable that mutations at the splice donor site of exon 29 and at the splice acceptor site of exon 13 have each been reported twice to cause multiple exon skipping. This suggests that these two exons predispose to multiple exon skipping in the presence of a splice site mutation.

In the index mutation, we supposed that the double exon skipping was due to the short length of intron 14 (107 bp). However, *in vitro* splicing of the minigene with an intact intron 14 failed to produce double exon skipping (Fig. 2). This indicated that the short length of intron 14 is not the sole determinant of multiple exon skipping. Remarkably, the time-course analysis of minigene splicing revealed that splicing of the middle intron, intron 14, occurred first for all four minigenes (Fig. 3). Because the structure of the intron and neighboring exons was accurate in the minigenes, we presume that intron 14 is spliced out at an early stage also *in vivo*. It is supposed that, in the patient's muscle, the removal of intron 14 is the major splicing event in the early stages, and then the splicing machinery identifies the splice acceptor site of exon 16 and the donor site of intron 13, thereby promoting the skipping of the two consecutive exons 14 and 15. As a minor pathway, the splicing machinery identifies the splice acceptor site of exon 15 and the donor site of intron 13, leading to exon 14 skipping.

Multiple splicing outcomes were exemplified for minigenes with transversion mutations but not for the minigene with a transition mutation (Fig. 2). Although a multiplicity of splicing outcomes was demonstrated *in vitro* as *in vivo*, the actual splicing patterns were different: a splicing intermediate retaining intron A was a major product *in vitro* (Fig. 2), whereas exon-skipped mature mRNAs were the main products *in vivo* (Fig. 1). Among the four *in vitro* splicing reactions, only the minigene with the G > C mutation produced exon 14-skipped mRNA. Even though the two transversion mutations both exerted drastic changes (Fig. 2), each produced different splicing outcomes. It is difficult to explain this difference. We conclude that both transversion mutations cause drastic changes in the splicing machinery and multiple splicing outcomes, but the identity of the substituted nucleotide induces the splicing pattern differences.

Recently, the manipulation of dystrophin pre-mRNA splicing is attracting much attention as a way to treat DMD (Matsuo, 1996; van Deutekom and van Ommen, 2003). AOs against splicing regulatory elements have been shown to induce exon skipping, thereby enhancing dystrophin expression in DMD patients (Takeshima *et al.*, 2006; van Deutekom *et al.*, 2007). Our results flag the possibility of multiple splicing outcomes after manipulation of splicing with AOs. Particular caution should be exercised when inducing skipping of the exons that have been reported to induce multiple exon skipping in the presence of a splice site mutation (Tuffery-Giraud *et al.*, 2004, 2005; Deburgrave *et al.*, 2007; Taylor *et al.*, 2007; Takeshima *et al.*, 2010). Considering that even a single-nucleotide change within exon sequence has been shown to induce splicing error (Shiga *et al.*, 1997; Nishiyama *et al.*, 2008), AO is supposed to induce unwanted splicing outcomes, such as activation of cryptic splice site created by new junction. In establishing exon skipping therapy with AO, therefore, splicing outcomes should be carefully monitored.

Acknowledgments

The authors thank Professor Peter K. Rogan for his encouraging support and Ms. Kanako Yokoyama for her secretarial help. This work was supported in part by a Grant-in-Aid for Scientific Research (B) and Grant-in-Aid for Exploratory Research from the Japan Society for the Promotion of Science; a Health and Labor Sciences Research Grant for Research on Psychiatric and Neurological Diseases and Mental Health; and a research grant for Nervous and Mental Disorders from the Ministry of Health, Labor, and Welfare, Japan.

Disclosure Statement

No competing financial interests exist.

References

Adachi K, Takeshima Y, Wada H, *et al.* (2003) Heterogous dystrophin mRNAs produced by a novel splice acceptor site mutation in intermediate dystrophinopathy. Pediatr Res 53: 125–131.

Ahn AH, Kunkel LM (1993) The structural and functional diversity of dystrophin. Nat Genet 3:283–291.

Bartolo C, Papp AC, Snyder PJ, *et al.* (1996) A novel splice site mutation in a Becker muscular dystrophy patient. J Med Genet 33:324–327.

Deburgrave N, Daoud F, Llense S, *et al.* (2007) Protein- and mRNA-based phenotype-genotype correlations in DMD/BMD with point mutations and molecular basis for BMD with nonsense and frameshift mutations in the DMD gene. Hum Mutat 28:183–195.

Den Dunnen JT, Grootscholten PM, Bakker E, *et al.* (1989) Topography of the Duchenne muscular dystrophy (DMD) gene: FIGE and cDNA analysis of 194 cases reveals 115 deletions and 13 duplications. Am J Hum Genet 45:835–847.

Habara Y, Doshita M, Hirozawa S, *et al.* (2008) A strong exonic splicing enhancer in dystrophin exon 19 achieve proper splicing without an upstream polypyrimidine tract. J Biochem 143:303–310.

Habara Y, Takeshima Y, Awano H, *et al.* (2009) *In vitro* splicing analysis showed that availability of a cryptic splice site is not a determinant for alternative splicing patterns caused by +1G—>A mutations in introns of the dystrophin gene. J Med Genet 46:542–547.

Hagiwara Y, Nishio H, Kitoh Y, *et al.* (1994) A novel point mutation (G^{-1} to T) in a 5′ splice donor site of intron 13 of the dystrophin gene results in exon skipping and is responsible for Becker muscular dystrophy. Am J Hum Genet 54:53–61.

Hertel K (2008) Combinatorial control of exon recognition. J Biol Chem 283:1211–1215.

Keren H, Lev-Maor G, Ast G (2010) Alternative splicing and evolution: diversification, exon definition and function. Nat Rev Genet 11:345–355.

Licatalosi DD, Darnell RB (2010) RNA processing and its regulation: global insights into biological networks. Nat Rev Genet 11:75–87.

Matsuo M (1996) Duchenne/Becker muscular dystrophy: from molecular diagnosis to gene therapy. Brain Dev 18:167–172.

Matsuo M, Masumura T, Nakajima T, *et al.* (1990) A very small frame-shifting deletion within exon 19 of the Duchenne muscular dystrophy gene. Biochem Biophys Res Commun 170: 963–967.

Matsuo M, Masumura T, Nishio H, *et al.* (1991) Exon skipping during splicing of dystrophin mRNA precursor due to an intraexon deletion in the dystrophin gene of Duchenne muscular dystrophy Kobe. J Clin Invest 87:2127–2131.

Monaco AP, Bertelson CJ, Liechti-Gallati S, *et al.* (1988) An explanation for the phenotypic differences between patients bearing partial deletions of the DMD locus. Genomics 2: 90–95.

Nishio H, Takeshima Y, Narita N, *et al.* (1994) Identification of a novel first exon in the human dystrophin gene and of a new promoter located more than 500 kb upstream of the nearest known promoter. J Clin Invest 94:1037–1042.

Nishiyama A, Takeshima Y, Zhang Z, *et al.* (2008) Dystrophin nonsense mutations can generate alternative rescue transcripts in lymphocytes. Ann Hum Genet 72:717–724.

Roberts RG, Barby TF, Manners E, *et al.* (1991) Direct detection of dystrophin gene rearrangements by analysis of dystrophin mRNA in peripheral blood lymphocytes. Am J Hum Genet 49:298–310.

Senapathy P, Shapiro MB, Harris NL (1990) Splice junctions, branch point sites, and exons: sequence statistics, identification, and applications to genome project. Methods Enzymol 183:252–278.

Shiga N, Takeshima Y, Sakamoto H, *et al.* (1997) Disruption of the splicing enhancer sequence within exon 27 of the dystrophin gene by a nonsense mutation induces partial skipping of the exon and is responsible for Becker muscular dystrophy. J Clin Invest 100:2204–2210.

Surono A, Takeshima Y, Wibawa T, *et al.* (1999) Circular dystrophin RNAs consisting of exons that were skipped by alternative splicing. Hum Mol Genet 8:493–500.

Takeshima Y, Yagi M, Okizuka Y, *et al.* (2010) Mutation spectrum of the dystrophin gene in 442 Duchenne/Becker muscular dystrophy cases from one Japanese referral center. J Hum Genet 55:379–388.

Takeshima Y, Yagi M, Wada H, *et al.* (2006) Intravenous infusion of an antisense oligonucleotide results in exon skipping in muscle dystrophin mRNA of Duchenne muscular dystrophy. Pediatr Res 59:690–694.

Taylor PJ, Maroulis S, Mullan GL, *et al.* (2007) Measurement of the clinical utility of a combined mutation detection protocol in carriers of Duchenne and Becker muscular dystrophy. J Med Genet 44:368–372.

Thi Tran HT, Takeshima Y, Surono A, *et al.* (2005) A G-to-A transition at the fifth position of intron 32 of the dystrophin gene inactivates a splice donor site both *in vivo* and *in vitro*. Mol Genet Metab 85:213–219.

Tuffery-Giraud S, Chambert S, Demaille J, *et al.* (1999) Point mutations in the dystrophin gene: evidence for frequent use of cryptic splice sites as a result of splicing defects. Hum Mutat 14:359–368.

Tuffery-Giraud S, Saquet C, Chambert S, *et al.* (2004) The role of muscle biopsy in analysis of the dystrophin gene in Duchenne muscular dystrophy: experience of a national referral centre. Neuromuscul Disord 14:650–658.

Tuffery-Giraud S, Saquet C, Thorel D, *et al.* (2005) Mutation spectrum leading to an attenuated phenotype in dystrophinopathies. Eur J Hum Genet 13:1254–1260.

van Deutekom J, Janson A, Ginjaar I, *et al.* (2007) Local dystrophin restoration with antisense oligonucleotide PRO051. N Engl J Med 357:2677–2686.

van Deutekom JC, van Ommen GJ (2003) Advances in Duchenne muscular dystrophy gene therapy. Nat Rev Genet 4:774–783.

Wimmer K, Roca X, Beiglböck H, *et al.* (2007) Extensive *in silico* analysis of NF1 splicing defects uncovers determinants for splicing outcome upon 5′ splice-site disruption. Hum Mutat 28:599–612.

Address correspondence to:
Masafumi Matsuo, M.D., Ph.D.
Department of Pediatrics
Graduate School of Medicine
Kobe University
7-5-1 Kusunokicho
Chuo-ku
Kobe 650-0017
Japan

E-mail: matsuo@kobe-u.ac.jp